AD-A047 918 GENERAL RESEARCH CORP SANTA BARBARA CALIF F/G 17/2.1
THE ROSCOE MANUAL. VOLUME 20 - SATELLITE COMMUNICATION MODEL.(U)
JAN 77 H S OSTROWSKY, J R GARBARINO DNA001-74-C-0182
UNCLASSIFIED CR-1-520-VOL-20 DNA-3964F-20 NL

1 OF 1
AD A047918

END
DATE FILMED
1 -78
DDC

DNA 3964F-20

THE ROSCOE MANUAL.

Volume 20-Satellite Communication Model

General Research Corporation
P.O. Box 3587
Santa Barbara, California 93105

Jan[redacted]1977

68p.

CR-1-520-Vol-20

Final Report.

DNA001-77-C-0182

CONTRACT No. DNA 001-74-C-0182

S99QAXH

Q964

APPROVED FOR PUBLIC RELEASE;
DISTRIBUTION UNLIMITED.

DNA, SBIE

3964F-20, AD-E300 046

THIS WORK SPONSORED BY THE DEFENSE NUCLEAR AGENCY UNDER RDT&E RMSS CODES B322074464 S99QAXHC06428 AND B322075464 S99QAXHC06432 H2590D.

H. S. Ostrowsky, J. R. Garbarino
J. J. Baltes

Prepared for

Director
DEFENSE NUCLEAR AGENCY
Washington, D. C. 20305

Destroy this report when it is no longer needed.
Do not return to sender.

UNCLASSIFIED

SECURITY CLASSIFICATION OF THIS PAGE (When Data Entered)

REPORT DOCUMENTATION PAGE

READ INSTRUCTIONS BEFORE COMPLETING FORM

1. REPORT NUMBER: DNA 3964F-20
2. GOVT ACCESSION NO.:
3. RECIPIENT'S CATALOG NUMBER:

4. TITLE (and Subtitle):
THE ROSCOE MANUAL
Volume 20—Satellite Communication Model

5. TYPE OF REPORT & PERIOD COVERED: Final Report

6. PERFORMING ORG. REPORT NUMBER: CR-1-520, Vol. 20

7. AUTHOR(s):
H. S. Ostrowsky
J. R. Garbarino
J. J. Baltes

8. CONTRACT OR GRANT NUMBER(s): DNA 001-74-C-0182

9. PERFORMING ORGANIZATION NAME AND ADDRESS:
General Research Corporation
P.O. Box 3587
Santa Barbara, California 93105

10. PROGRAM ELEMENT, PROJECT, TASK AREA & WORK UNIT NUMBERS:
Subtasks S99QAXHC064-28
and S99QAXHC064-32

11. CONTROLLING OFFICE NAME AND ADDRESS:
Director
Defense Nuclear Agency
Washington, D. C. 20305

12. REPORT DATE: January 1977

13. NUMBER OF PAGES: 72

14. MONITORING AGENCY NAME & ADDRESS (if different from Controlling Office):

15. SECURITY CLASS. (of this report): UNCLASSIFIED

15a. DECLASSIFICATION/DOWNGRADING SCHEDULE:

16. DISTRIBUTION STATEMENT (of this Report):
Approved for public release; distribution unlimited

17. DISTRIBUTION STATEMENT (of the abstract entered in Block 20, if different from Report):

18. SUPPLEMENTARY NOTES:
This work sponsored by the Defense Nuclear Agency under RDT&E RMSS Codes B322074464 S99QAXHC06428 and B322075464 S99QAXHC06432 H2590D.

19. KEY WORDS (Continue on reverse side if necessary and identify by block number):

Nuclear Effects	Propagation
Radar	Satellite Communication
Computer Program	Simulation

20. ABSTRACT (Continue on reverse side if necessary and identify by block number):
The ROSCOE computer code is designed specifically to be the "laboratory standard" for evaluating nuclear effects on radar and optical sensors. The program provides a means for (1) evaluating radar acquisition, discrimination, and tracking performance in a nuclear environment; (2) estimating various radar and optical propagation error sources; and (3) computing specific phenomenological data. Volume 20 of this series describes ROSCOE's satellite communication model.

DD FORM 1 JAN 73 1473 EDITION OF 1 NOV 65 IS OBSOLETE

UNCLASSIFIED

SECURITY CLASSIFICATION OF THIS PAGE (When Data Entered)

CONTENTS

1 INTRODUCTION

The ROSCOE Communication Model is a computer program that combines the ROSCOE nuclear phenomenology and propagation modules with a package that simulates a communication link and computations specific to four types of digital modulation. These are: binary frequency shift keying (FSK), both coherent and non-coherent, and binary phase shift keying (PSK), both coherent and differentially coherent. These four were selected because they are applicable to a large number of satellite communication systems, both current and future, and because mathematical models of these processes are readily available in the literature.

In addition to the choice of modulation, the user has a wide range of options in setting up the link parameters. He may select antenna types, beam patterns and gains, RF frequencies, bandwidths, transmitter powers, receiver noise factors, line losses, and bit rates. He may select either plain amplification or regeneration (i.e., demodulation and retransmission) of the signal at the satellite transponder. The "ground" stations may be either stationary or mobile, and may be airborne. If (as is usually the case) the receiver filters are not perfectly matched to the signals, the appropriate mismatch losses will be calculated. If one or more of the antennas are phased arrays, the off-boresight scanning loss will be computed. All of these are applicable individually to the uplink and downlink and separately to each antenna, transmitter, and receiver in the system.

The environmental effects which are modeled include losses due to absorption (both nuclear-induced and ambient), refractive beam-spreading, and dispersion (additional filter mismatch at the receivers), external noise due to nuclear sources, atmospheric absorptive effects, galactic sources, the earth, and the sun. Also included are correlated amplitude and phase scintillations due to striations. The amplitude scintillations (fades) affect all types of signal modulation through the signal-to-noise ratios at the receivers; the specific effects of the phase scintillations

on demodulator performance are considered in detail for the PSK modulations. The most complete model is available for the case of DPSK, where the user can also choose either to average the effect of the instantaneous phase scintillations over the ensemble of possible phase errors or to select a (correlated) random sample from this ensemble at each calculation.

This memorandum briefly describes the mathematical models contained in the ROSCOE Communication Model. Although the sources are indicated whenever possible, no attempt has been made to derive or justify these formulae and algorithms. To do so would have multiplied the length of this document several fold.

2 THE FUNDAMENTAL PARAMETER

The fundamental parameter which can be used to determine the properties of a digital communication link is γ, the ratio of the total average received energy per signal element to the noise power per unit bandwidth:

$$\gamma = E/N_o \tag{1}$$

This can also be expressed in terms of other important properties of the link by noting that

$$\gamma = \left(\frac{S}{N}\right)\tau B \equiv \left(\frac{S}{N}\right)\frac{B}{\rho}\log_2 M \tag{2}$$

where $\left(\frac{S}{N}\right)$ = received signal-to-noise ratio

τ = length of a signal element, seconds

B = receiver IF bandwidth, Hz

ρ = data transmission rate, bits/second

M = number of possible waveforms per transmission: for an M-ary system,

$$\rho \equiv \frac{\log_2 M}{\tau} \tag{3}$$

The dependence of γ on the basic system and propagation parameters can be made explicit by recalling that

$$\left(\frac{S}{N}\right) = \frac{P_t G_t G_r \lambda^2}{(4\pi)^2 R^2 L L_1 L_2 k B (T_n + T_x)} \tag{4}$$

where P_t = total average radiated RF power at transmitting antenna

G_t = gain of transmitting antenna

G_r = gain of receiving antenna

λ = wavelength of transmitted carrier

R = distance between transmitting and receiving antennas

L = total propagation loss between transmitting and receiving antennas

L_1 = system loss between transmitter and transmitting antenna

L_2 = line loss between receiving antenna and receiver

k = Boltzmann's constant

B = receiver IF bandwidth

T_n = nominal system noise temperature

T_x = receiver noise temperature due to all external noise *sources*

The two temperatures appearing in this equation are further defined by

$$T_n \equiv T_R + \left(\frac{L_2 - 1}{L_2}\right)T_p \equiv (\overline{NF} - 1)T_o + \left(\frac{L_2 - 1}{L_2}\right)T_p \qquad (5)$$

and

$$T_x \equiv \frac{T_A}{L_2} \qquad (6)$$

where T_R = receiver noise temperature

T_p = physical temperature of antenna

$\overline{NF}$ = receiver noise figure

T_o = reference temperature ($T_o = 290°K$)

T_A = antenna noise temperature due to all external noise sources

Finally, it is assumed that both link antennas are steerable reflectors pointing directly at one another. If either of the antennas is a phased array, then Eq. 4 must be altered by replacing the appropriate gain factor, G, by $G_o \cos\theta$, where G_o is the boresight gain of the phased array antenna and θ is the current off-boresight beam pointing angle.

All of this excruciating detail has been given here because this set of equations determines how the communication system and the propagation environment interact to produce the fundamental parameter. All propagation effects can be described by stating how they affect either L or T_A, and any additional losses caused by demodulator performance in an imperfect environment are functions of the received value of γ before demodulation.

The present version of the ROSCOE Communication Model considers binary systems only. Thus $M \equiv 2$ and $\rho \equiv 1/\tau$. Furthermore, it might be worth noting that the time-bandwidth product is generally a number of the order of unity: $\tau B \sim 1$.

3 PROBABILITY OF ELEMENT ERROR

The measure of overall system performance used in the ROSCOE Communication Model is P_e, the probability of element error. Recall that a digital signal consists of a sequence of symbols, each of which is made up of a sequence of elements. For each received element (including spaces) in the message the receiver makes a judgment, based on tests which are specific to the particular signaling mode being used, as to which element was transmitted. The probability that the receiver will make a wrong judgment on a given element is P_e. If $M > 2$ each element conveys more than one bit of information, so in general P_e is not the same thing as the probability of bit error. For $M = 2$ the distinction vanishes.

Of course, appropriate coding can be used to reduce the incidence of message errors even when P_e is not insignificant, but coding is a complex subject with which we shall not be concerned here. The element error probability, P_e, is the final output of each calculation in the Communication Model.

For each of the binary digital modulation modes contained in the present ROSCOE model, there is a simple closed-form expression for P_e as a function of γ alone, which can be found in standard texts on communication theory such as Ref. 1. These are:

Coherent Phase-Shift Keying (CPSK)

$$P_e = \frac{1}{2} \operatorname{erfc} \sqrt{\gamma} \tag{7a}$$

Differentially Coherent Phase-Shift Keying (DPSK)

$$P_e = \frac{1}{2} \exp(-\gamma) \tag{7b}$$

Coherent Frequency-Shift Keying (CFSK)

$$P_e = \frac{1}{2} \operatorname{erfc} \sqrt{\frac{\gamma}{2}} \tag{7c}$$

Non-Coherent Frequency-Shift Keying (NFSK)

$$P_e = \frac{1}{2} \exp\left(-\frac{\gamma}{2}\right) \tag{7d}$$

where $\operatorname{erfc}(x) \triangleq 1 - \operatorname{erf}(x)$

Since these simple expressions involve only γ, they obviously cannot account for any possible dependence of P_e on other variables. As such they are strictly valid only for isolated single elements in an environment which is changing very slowly (or not at all) relative to the element length. For more rapid, but still sufficiently slow, amplitude variations (slow fading) they can be modified by integrating over the probability distribution function in γ, if known. The resulting expressions would then represent an average P_e over a time period encompassing many fades, and would no longer be appropriate for a deterministic single-pulse model. When phase fluctuations become significant, as is usually the case when propagation through a striated medium occurs, even more complicated modifications are necessary. For PSK systems the appropriate modifications have been found in the literature and incorporated into the ROSCOE model. For FSK, such modifications have not been available and are not included.

It should be emphasized that Eqs. 7 are useful starting points for further analysis, and provide good baseline computations even in unmodified form.

4 AMPLIFICATION OR REGENERATION

Satellite communication is almost always a process in which two different stations on (or near) earth contact one another by way of a satellite station as intermediary. The complete path of communication, then, involves both an uplink and a downlink, each affected by its individual propagation environment. Each link therefore will have its own value of P_e which will, however, have only a potential existence unless the signal is actually demodulated upon reception at the link terminus.

The ROSCOE Communication Model calculates the values of P_e for the uplink and the downlink and also for the total up-and-down communication path. The way in which the total P_e for the received signal is determined depends on how the uplink signal is processed at the satellite before retransmission to earth. There are fundamentally two ways this can be done: amplification or regeneration. The ROSCOE model permits the user to select one or the other of these alternatives; they are, of course, mutually exclusive in any given transmission.

The satellite transponder can amplify and retransmit the incoming signal without ever demodulating it. In that case, neither the potential $P_e(\text{up})$ nor the potential $P_e(\text{down})$ have an actual existence; only the $P_e(\text{total})$ exists and is calculated by means of an appropriate equation (e.g., Eqs. 7) as a function of $\gamma(\text{total})$. Letting γ_u and γ_d be the fundamental parameters for the uplink and downlink, respectively, it is not difficult to show that

$$\gamma(\text{total}) = \left[\frac{B_u T_u}{B_d T_d}\frac{1}{\gamma_u} + \frac{1}{\gamma_d}\right]^{-1} \tag{8}$$

where $B_u T_u$ and $B_d T_d$ are the respective time-bandwidth products.

On the other hand, if regeneration is used, then the satellite transponder first demodulates the incoming signal, then imposes an equivalent modulation on a new signal which is transmitted down to earth. Now, both $P_e(\text{up})$ and $P_e(\text{down})$ have concrete existence and meaning, and the value of $P_e(\text{total})$ must be calculated by carefully combining them in proper fashion. The correct combination depends on the value of M for the system; since we are concerned at present only with binary systems, it is easily seen that

$$P_e(\text{total}) = P_e(\text{up}) + P_e(\text{down}) - 2P_e(\text{up}) \cdot P_e(\text{down}) \qquad (9)$$

5 PROPAGATION AND THE ENVIRONMENT

On its way from transmitter to receiver the signal is affected or acted upon by the environment through which it propagates. These effects show up as loss factors to be multiplied into L, as antenna temperatures to be added to T_A, and as phase fluctuations which affect some types of communication systems in more complicated ways. Some are specifically related to the nuclear bursts and associated phenomena: smoothly-varying absorption (appearing as a loss factor L_A), fluctuating absorption due to striations (appearing as correlated fades changing the value of γ), beam-spreading loss (L_B), dispersive loss (L_D), fireball noise (T_F), and phase scintillations with variance μ^2 and decorrelation time τ_D. Some are related to the natural environment: tropospheric absorption (L_T), ionospheric absorption (included as part of L_A), noise due to atmospheric oxygen and water vapor (T_T), solar radiation (T_S), galactic radiation (T_G), and the earth's effective radiating temperature (T_E). All of these will be described briefly in the following subsections.

5.1 NUCLEAR AND IONOSPHERIC EFFECTS

A stochastic calculation of the effects of the ionosphere and any nuclear fireballs or debris regions on signals propagating through them may be thought of as the pivotal element in the ROSCOE Communication Model, comprising as it does the meeting place of the nuclear phenomenology, signal propagation, and system aspects of the model. This is not the place, however, to discuss the details of these calculations, which may be found elsewhere.[2] ROSCOE contains modules that calculate the electron density along the path; the locations, directions, size and density distributions, and motions of striated regions; and refractive propagation through smooth or striated media. Combining these data with the locations, properties, and motions of the transmitting and receiving antennas, it is possible to compute values for the simple absorption (L_A), beam-spreading loss (L_B), RMS phase scintillations (μ), scintillation decorrelation time (τ_D), and integrated electron density (I_E) along the path between these antennas at any given time. It should be noted

that this calculation includes the effects of both dispersive time delays and dog-leg multipaths on the phase error variations, and therefore differs from some of the simpler models found in the literature, which include only the former.

Another calculation based on the nuclear phenomenology provides a value for the effective integrated fireball thermal noise temperature (T_F) as seen by the receiving antenna for the given link. This model involves the sizes, shapes, temperatures, emissivities, motions, and locations of all contributing fireballs, the attenuation along the paths connecting them to the receivers, and the appropriate beam-filling factors related to the size, shape, and location of the antenna beam.

5.2 DISPERSIVE LOSSES

When propagating through an ionized medium, a time-limited signal experiences dispersion, which alters its spectral content. If such a signal is then put through a receiver filter which is matched to the original transmitted form, there will be a mismatch and consequent energy decrease which we can express as a dispersive loss. Two distinct losses of this type are included in ROSCOE by means of simplified but generally adequate models.

The original signal element is idealized as a rectangular pulse of length τ, and the receiver filter is idealized as a rectangular bandpass filter of bandwidth B. Even if there is no dispersion, such a filter is not really a match to the signal, so there will always be some mismatch loss, L_F. For PSK modulations this primary mismatch loss is represented by $L_F = 1/\eta_o$, where η_o is defined by Eq. 20' in Sec. 6.1. The analysis leading up to the definition of η presented in that section is pretty complicated. For FSK modulations, a simpler form of analysis is used which in effect considers isolated single signal elements and ignores the alterations due to coupling of quasi-random trains of such pulses in real signals. The primary mismatch loss can then be shown to be given by

$$L_F = \frac{\pi}{2} \frac{x}{[Si(x)]^2} \tag{10}$$

where

$$x \equiv \frac{\pi}{2} \tau B \tag{11}$$

It is well known that the loss function of Eq. 10 has a broad minimum at $x \simeq 2.2$ (equivalent to $\tau B \simeq 1.4$), at which point the mismatch loss is approximately $L_F \simeq 1.2$ (0.8 dB). If the filter bandwidth differs from this optimum value the loss factor will be accordingly greater.

If in addition the signal experiences dispersion through traversal of an ionized region characterized by a total integrated electron density of I_E, then there is an additional dispersive loss. By making a quadratic approximation to the dispersion function, it is not difficult to find an expression for this dispersive loss factor; it turns out to be

$$L_D = \frac{\pi}{2} \frac{x}{L_F} \frac{1}{G(a,x)} \tag{12}$$

where

$$G(a,x) \equiv \left| \int_0^x \frac{\sin \xi}{\xi} \exp\left(i \frac{a^2 \xi^2}{4} \right) d\xi \right|^2 \tag{13}$$

and

$$a = \frac{0.06 I_E^{1/2}}{\tau f^{3/2}} \tag{14}$$

f being the carrier frequency (Hz). This approximation is used in the ROSCOE model.

5.3 TROPOSPHERIC AND CELESTIAL EFFECTS

As the signal traverses the troposphere, it is subject to a loss, L_T, due to absorption by oxygen and water vapor. The downlink antenna also receives a noise component, designated by T_T, due to reradiation by oxygen and water vapor. The calculation of these two effects is based on curve fits to empirical data on these two phenomena, as functions of antenna elevation angle and carrier frequency. These models were taken directly from the SATL code,[3] and will not be reproduced here.

There are also noise components, in one or the other receiving antenna, due to "celestial" sources, namely the sun, the galactic background, and the earth as a radiator. For most frequencies of interest to satellite communication systems these are relatively small temperature increments, and their values can only be approximated since conditions vary with time and location. Nevertheless, approximations to these three antenna temperatures have been included in ROSCOE in the interest of completeness.

The uplink receiving antenna, looking down upon the earth, does not see the sun or the galaxy. It sees the earth's surface, radiating a noise whose power can be related to an antenna temperature, T_E. This noise, which comes originally from the surface but is transferred to the satellite antenna by way of reradiation through the atmosphere, should be a function of frequency f. However, we have not been able to find data on this phenomenon, so in the present ROSCOE model we have substituted a constant temperature, approximately that of the upper atmosphere, namely $T_E = 250°$. If a more realistic model should come to our attention it can easily be substituted for this approximation, which in the meanwhile we retain.

The downlink receiving antenna, looking up, receives radiation from the general galactic background, and from the sun if some portion of the antenna's mainlobe intersects the solar disk. The ROSCOE models for these phenomena are taken from a paper by Hogg and Mumford.[4]

The received cosmic noise from the galaxy appears as from a continuous source covering a large area of the sky, but having an intensity which varies with angular distance from the galactic center as well as with the carrier frequency. There are also, of course, localized cosmic sources (radio stars, quasars, etc.), but it would not be practical to include a map of their locations in the ROSCOE model, so they are ignored. Similarly, the variations in galactic noise temperature with celestial latitude and longitude involve more calculational complexity than is warranted by the importance of the result. This is replaced by an approximate average temperature which is a function only of the frequency:

$$T_G \simeq \frac{2.6 \times 10^{19}}{f^2} \ ^\circ K \tag{15}$$

The noise temperature of the sun depends somewhat on the time within the sunspot cycle, as well as localized phenomena such as flares. Ignoring this, we will use the mean temperature of the quiet sun, which is a function only of frequency. Empirical data are well fitted by the following approximations:

For $f < 250$ MHz or $f > 35$ GHz ,

$$T_\odot \simeq \frac{2 \times 10^{14}}{f} \ ^\circ K \tag{16a}$$

For $250 \text{ MHz} \leq f \leq 35 \text{ GHz}$,

$$T_{\odot} = \frac{2 \times 10^{14}}{f} \left\{ 1 + \frac{1}{2.3} \sin \left[2\pi \log 2.6 \left(f \times 10^{-9} - 0.10 \right) \right] \right\} \qquad (16b)$$

the frequency f being given in Hz.

Unless the solar disk completely fills the radar beam, however, this is not the antenna temperature seen by the receiver. In order to find T_S it is necessary to multiply $T_{\odot}$ by a beam-filling factor which depends on the size and location of the antenna beam relative to the sun. If the solar disk is completely outside the mainlobe, the beam-filling factor is approximated by zero; otherwise, it is computed by a straightforward but complicated little algorithm which need not be reproduced here.

6 SCINTILLATIONS AND STRIATIONS

If the environment remains constant or varies slowly in a smooth manner, the computations already described are sufficient to complete the model. The presence of striations and the attendant scintillations introduces new difficulties which must be dealt with. Propagation through a region of field-aligned striations is known to introduce phase fluctuations, often of considerable magnitude. At a sufficient distance from the striated region ("phase screen") these can add up to produce significant amplitude fluctuations as well, although it is not uncommon to find little or no amplitude fluctuation at a place where the phase is scintillating greatly.

This is not the place to go into the extensive literature on the origins and properties of these scintillations. In any case there is not yet a general consensus on this subject, and the debate in the literature continues to be sometimes heated. What is needed for ROSCOE is a model which is in good agreement with experimental data or theoretical findings for such cases as are widely acceptable by the community, which produces reasonable results for cases where understanding remains obscure, and which passes smoothly from one regime to the other. It is desirable to make as few ad hoc assumptions as possible.

Let us consider now the modeling of the effects of phase and amplitude scintillations on the digital communication systems.

6.1 PHASE SCINTILLATIONS

The ROSCOE propagation model produces a description of phase scintillations which is stochastic rather than deterministic. The correlated phase fluctuations at the receiving antenna are represented by a zero-mean, stationary Gaussian process with variance μ^2 and decorrelation time τ_D. From these two quantities it is possible to build up a picture of how a PSK communication system will be affected by the phase scintillations. This analysis has been very well described in two ESL

reports,[5,6] upon which this part of the ROSCOE model is primarily based. Although we will quote the needed results in this subsection, the reader is referred to the original reports for details.

As far as FSK communications systems are concerned, we have no information on possible effects of phase scintillations on them, and the ROSCOE model does not contain any such effects.

Returning to the statistical model presented in the ESL reports, it is assumed that the phase scintillation process is represented by a first-order Butterworth power spectral density (PSD) function:

$$S_{\psi}(\omega) = \frac{2\mu^2/\tau_D}{\omega^2 + (1/\tau_D)^2} \tag{17}$$

corresponding to an exponential autocorrelation function of the form

$$R_{\psi}(t) = \mu^2 e^{-|t|/\tau_D} \tag{18}$$

The two-sided PSD of the PSK modulated signal with the random phase scintillations imposed on it is called $S_s(f)$ and is given by a complicated expression which we shall not attempt to reproduce here. When the signal is passed through the receiver's band-pass filter (of bandwidth B), it can be shown that the signal-to-noise ratio after filtering is reduced by a factor η as compared to its value prior to the filter. The factor η is defined by

$$\eta(\tau B, \tau/\tau_D, \mu) \equiv \frac{4}{A^2} \int_{f_o - B/2}^{f_o + B/2} S_s(f)\, df \tag{19}$$

where A is the amplitude and f_o the frequency of the signal carrier. This factor η is quite important for the rest of this analysis. In addition to expressing the SNR loss due to IF filtering prior to demodulation, we shall also see it appear in the analysis of the performance of a CPSK demodulator.

With a considerable amount of effort, the integral in Eq. 19 can be reduced to a series whose form, however, is not particularly transparent. It is:

$$\eta(\tau B, \tau/\tau_D, \mu) = \frac{2}{\pi} e^{-\mu^2} \sum_{n=0}^{\infty} \frac{\mu^{2n}}{n!} f_n(\tau B, \tau/\tau_D) \tag{20a}$$

where

$$f_n \equiv \frac{\left[\pi B\tau \cos(\pi B\tau) + \frac{n\tau}{\tau_D} \sin(\pi B\tau)\right] e^{-n\tau/\tau_D} - \pi B\tau}{r_n^2}$$

$$+ \sum_{m=1}^{\infty} \frac{(-1)^m r_n^m \sin(m\theta_n^*)}{m \cdot m!} \tag{20b}$$

with

$$r_n \equiv \left[(\pi B\tau)^2 + \left(n \frac{\tau}{\tau_D}\right)^2\right]^{1/2} \tag{20c}$$

and

$$\theta_n^* \equiv -\tan^{-1}\left(\pi B\tau \cdot \frac{\tau_D}{n\tau}\right) \tag{20d}$$

As may well be imagined, the creation of a computer subroutine to evaluate this function η was a rather delicate matter.

It should be noted that when there are no scintillations ($\mu = 0$ or $\tau_D \to \infty$) the function η does not become unity, but takes on the value

$$\eta_o = \frac{2}{\pi}\left[S_i(\pi B\tau) - \frac{1 - \cos(\pi B\tau)}{\pi B\tau}\right] \tag{20'}$$

We have just seen that when PSK modulation is being used the signal-to-noise ratio, and hence also the fundamental parameter γ, prior to demodulation is reduced by the factor η. Therefore, when regeneration is being employed, the values of γ_u and γ_d (the subscripts standing for "uplink" and "downlink," respectively) must be replaced by $\eta_u\gamma_u$ and $\eta_d\gamma_d$ when evaluating the error probabilities $P_e(\text{up})$ and $P_e(\text{down})$.

When regeneration is <u>not</u> being employed, we must first determine the values of μ_T and τ_{DT} for the total composite path consisting of uplink and downlink (the subscript T standing for "total"). For the variance μ^2 the correct formulation is obvious:

$$\mu_T^2 = \mu_u^2 + \mu_d^2 \tag{21}$$

For the decorrelation time, however, the appropriate combination can only be estimated; we use the approximation

$$\tau_{DT} \approx \left[\frac{1}{\tau_{Du}} + \frac{1}{\tau_{Dd}}\right]^{-1} \tag{22}$$

We can now use these values to compute the factor η_T for the combined two-way path. Finally, it can be shown that the total received γ before demodulation at the ground receiver is given by

$$\gamma_T = \eta_T \left[\frac{B_u \tau_u}{B_d \tau_d} \frac{1}{\eta_u \gamma_u} + \frac{1}{\gamma_d} \right]^{-1} \tag{23}$$

which may be compared to Eq. 8 where the effect of the loss factor η was not yet known. The probability of element error, P_e(total) , is computed using this γ_T.

The calculation of P_e , however, is not now done by means of Eqs. 7a and 7b for PSK modulations. These are replaced by more complicated forms taking into account the effects of the phase scintillations on the demodulator performance. Again, the complete analyses are found in the ESL documents previously referenced; here only the results are stated.

For DPSK we first define the amplitude parameter,

$$\alpha \equiv \sqrt{2\gamma} \tag{24}$$

and the variance of the phase difference between successive elements,

$$\sigma_\phi^2 \equiv 2\mu^2 \left[1 - \exp\left(- \frac{\tau}{\tau_D} \right) \right] \tag{25}$$

From this point there are two ways we can go; the ROSCOE model contains both and allows the user to select the one he prefers. If the calculation is desired to be as deterministic as possible, successive values of ϕ are chosen from the zero-mean Gaussian distribution of variance σ_ϕ^2 and substituted directly into the formula for P_e , which now has the form

$$P_e = \frac{1}{2} F(\alpha, \phi) \tag{26a}$$

where

$$F(\alpha,\phi) \equiv 1 - Q\left(\alpha \cos\frac{\phi}{2}\ ,\ \alpha \sin\frac{\phi}{2}\right) + Q\left(\alpha \sin\frac{\phi}{2}\ ,\ \alpha \cos\frac{\phi}{2}\right) \tag{26b}$$

$Q(a,b)$ being Marcum's "Q-Function."[7]

The successive values of ϕ used in this expression are computed in such a way as to remain approximately correlated, with a decorrelation time τ_D. This is done by the usual two-point approximation, as follows: let the first value in this sequence, ϕ_1, be chosen directly from the Gaussian distribution. The second member of the sequence is found by choosing a new ϕ' from the Gaussian distribution and computing the combination

$$\phi_2 = F\phi_1 + \sqrt{1 - F^2}\ \phi' \tag{27}$$

where

$$F \equiv e^{-\Delta t/\tau_D} \tag{28}$$

Δt being the time interval between sample 1 and sample 2. Succeeding values of ϕ are found by iterating this procedure:

$$\phi_n = F\phi_{n-1} + \sqrt{1 - F^2}\ \phi' \tag{27'}$$

with a new ϕ' (and F if necessary) each time.

If this quasi-deterministic model is not required, a mean value for P_e can be calculated instead by integrating the conditional

probability of error, $P_e(\phi)$, over the ensemble of all possible values of ϕ with their appropriate probabilities, i.e.,

$$\overline{P_e} = \frac{1}{\sqrt{2\pi}\,\sigma_\phi} \int_0^\infty F(\alpha,\phi)\, \exp\left[-\frac{\phi^2}{2\sigma_\phi^2}\right] d\phi \tag{29}$$

For CPSK systems the problem is more complicated because it is necessary to consider the phase-locked loop (PLL) in the demodulator. The phase error variance at the demodulator is the sum of two terms:

$$\sigma_\phi^2 = \sigma_{\phi n}^2 + \sigma_{\phi s}^2 \tag{30}$$

where $\sigma_{\phi n}^2$ is the variance due to noise alone in the PLL, and $\sigma_{\phi s}^2$ is the variance due to the phase scintillations in the PLL. It can be shown that

$$\sigma_{\phi n}^2 = \eta^2 \frac{B_L T}{\gamma}\left(1 + \frac{B_T}{2\gamma}\right) \tag{31}$$

where B_L is the noise bandwidth of the PLL.

This loop noise bandwidth can be an input quantity, but it is also possible to compute its value in terms of other constants which define the desired operating characteristics of the communication link. Thus, suppose the link has to have a probability of element error given by P_o, and that the RMS phase error in the loop due to noise alone cannot be reduced below σ_n (typically 5°-10°). In an ideal environment, the fundamental parameter, γ_o, which would be needed in order to achieve the given error rate could be calculated by inverting Eq. 7a in the form

$$P_o = \frac{1}{2}\,\mathrm{erfc}\sqrt{\gamma_o} \tag{32}$$

Then we can use Eq. 31 to find the desired loop noise bandwidth.

$$B_L = \frac{\gamma_o \sigma_n^2}{\eta_o^2 \tau} \frac{1}{1 + \frac{B\tau}{2\gamma_o}} \tag{33}$$

where η_o is the value of $\eta(B\tau, \tau/\tau_D, \mu)$ when there are no scintillations, i.e., as $\mu \to 0$ and $\tau_D \to \infty$.

Now we must find $\sigma_{\phi s}^2$, which can be expressed as an integral in the form

$$\sigma_{\phi s}^2 = \frac{1}{2\pi} \int_{-\infty}^{\infty} |1 - H(j\omega)|^2 S_\psi(\omega)\, d\omega$$

where $H(s)$ is the transfer function of the PLL and $S_\psi(\omega)$ is the PSD of the random phase modulation process. The form of $H(s)$, and thus of $\sigma_{\phi s}^2$, depends on the order of the PLL.[8] In the ROSCOE model the user may specify either a first-order loop or a second-order loop with damping factor ζ. It can then be shown that for a first-order PLL

$$\sigma_{\phi s}^2 = \frac{\mu^2}{1 + 4B_L \tau_D} \tag{34}$$

and for a second-order PLL with damping factor ζ

$$\sigma_{\phi s}^2 = \frac{\mu^2 (1 + aB_L \tau_D)}{1 + bB_L \tau_D + ab(B_L \tau_D)^2} \tag{35}$$

where

$$a \equiv \frac{4}{4\zeta^2 + 1} \tag{36a}$$

and

$$b \equiv \frac{16\zeta^2}{4\zeta^2 + 1} \tag{36b}$$

It ought to be mentioned that the most commonly employed compromise between stability and speed of response in a second-order PLL is to make the damping factor

$$\zeta \equiv 1/\sqrt{2}$$

Having found now the total variance of the PLL phase error, we can relate it to the probability of element error in the following way. It can be shown that the probability density distribution for the phase error of a PLL is

$$p(\phi) = \frac{e^{\alpha \cos \phi}}{2\pi I_o(\alpha)} \quad ; \qquad |\phi| \leq \pi \tag{37a}$$

where

$$\alpha \equiv 1/\sigma_\phi^2 \tag{37b}$$

and $I_o(x)$ is the modified Bessel function of the first kind and zero order. This equation is strictly correct only for a first-order PLL when the input is white noise plus a sine wave with Gaussian random phase modulation having the PSD shown in Eq. 17. However, Lindsey[9] has suggested

that this probability density should be adequate to represent second-order loops, also, in the region where they are usually operated, and uses Eq. 37 for the PLL of either order; we shall do likewise.

Now we can find the probability of element error by combining this with the formula for P_e for a CPSK system, as modified to take into account a phase error, ϕ, namely[10]

$$P_e(\phi) = \frac{1}{2} \operatorname{erfc}\left(\sqrt{\gamma \cos^2\phi}\right) \tag{38}$$

Averaged over the ensemble of possible phase errors, the mean element error probability is given by

$$\overline{P_e} = \frac{1}{2\pi I_o(\alpha)} \int_0^{\pi} \operatorname{erfc}\left(\sqrt{\gamma \cos^2\phi}\right) e^{\alpha \cos \phi} \, d\phi \tag{39}$$

If a quasi-deterministic, single-element value were desired, we could take correlated samples from the distribution of Eq. 37 for substitution into Eq. 38. This option is not available in the present version, but can be added without much difficulty.

6.2 AMPLITUDE SCINTILLATIONS

With respect to the amplitude scintillations caused by a striated medium, a more heuristic approach is unfortunately necessary, because no single theory or explanation is accepted as correct over the whole range of expected conditions. What we are seeking, for the ROSCOE model, is a simple computational algorithm which yields reasonable statistics for the fluctuating signal amplitude at all distances from the near field to the far field (relative to the striated region), and for all values of the phase error variance μ^2. We find that a great number of research papers have been published on aspects of this problem over the past 20

years. They are very definitely not in complete agreement, often are contradictory. Yet certain results, valid under specific different conditions, do seem to find general acceptance. We have proceeded from these benchmarks to induce an algorithm which agrees with them where they are valid and produces reasonable results when extended to regions where they are invalid. There is no contention here that the algorithm is "correct" or could be rigorously justified, only that it is reasonable and has the right values in limiting cases. Since the experimental measurements themselves have not generally been very precise, we see no need at this time to try for any more rigorous formulation.

The heuristic induction process, while interesting, does not belong to this memorandum and will not be described here. We will present only the necessary preliminaries and quote the conclusions. It may be worth indicating, however, that the sources and starting places for this work are to be found in papers by Mercier,[11] Briggs and Parkin,[12] Lawrence, Little, and Chivers,[13] Singleton,[14] Rino and Fremouw,[15] and Valley.[16]

Consider, now, a geometry where the transmitter is located on one side of a striated region (sometimes representable by a "phase screen") at a distance R_1 from it, and the receiver is located on the other side at a distance R_2. We define a new variable

$$Z \triangleq \frac{R_1 R_2}{R_1 + R_2} \tag{40}$$

We also define a parameter

$$Z_F \triangleq \frac{\pi r_o^2}{2\lambda} \tag{41}$$

where r_o is the transverse scale size of the striations. This Z_F is approximately equal to the "Fresnel distance" for these striations. When the striations are represented as having Chesnut's size distribution with $n = 6$ and parameter σ_o, then it can be shown that $r_o = 2\sigma_o$.

The quantity

$$x \equiv Z/Z_F \tag{42}$$

determines whether we are in the far field ($x >> 1$), the near field ($x << 1$), or as is very often the case, the transition region. In order to make this transition in a smooth manner we introduce the function (not to be confused with Marcum's "Q Function")

$$Q(x) \triangleq \frac{x^2}{1 + x^2} \tag{43}$$

Now suppose that in the absence of striations the signal would have had a fundamental parameter $\gamma = \gamma_1$ at the receiver. When the striations are present the value of γ will be increased and decreased in a time-correlated manner as the line of sight moves across the striations. To begin the computation of γ we define a normalized amplitude,

$$R_o \triangleq \sqrt{\frac{2\gamma_1}{\tau B}} \tag{44}$$

in the absence of striations.

Given that the striations produce phase scintillations with variance μ^2, we next define the parameter

$$A = \exp\left[-\frac{1}{2} Q(x)\mu^2\right] \tag{45}$$

This is the heart of the heuristic algorithm. The strength of the scintillations is essentially contained in the factor μ^2, while the factor $Q(x)$ takes care of the dependence on near-field/far-field distance. We introduce the normalized amplitudes

$$P \triangleq AR_o \tag{46a}$$

and

$$\sigma_T \triangleq \sqrt{1 - A^2}\, R_o \tag{46b}$$

Here, P is the amplitude of that portion of the signal which remains in the "specular" component and σ_T represents the "diffracted" component in the sense that σ_T^2 is the variance of this interference term. It will be noted that conservation of energy is satisfied, since $P^2 + \sigma_T^2 \equiv R_o^2$.

Now another complexity enters the picture. It is generally accepted that in the far field the in-phase component (σ_x) and the quadrature component (σ_y) of the "scintillation noise" are equal, i.e., as $x \to \infty$

$$\sigma_x^2 = \sigma_y^2 = \frac{1}{2}\sigma_T^2 \quad ,$$

and Rician[17] statistics are valid. At closer distances, there is evidence that more of the energy goes into the quadrature component at the expense of the in-phase component, i.e., for $x \lesssim 1$, $\sigma_y^2 > \sigma_x^2$.

To represent this phenomenon we make use of a result due to Valley.[16] Let it be stated at the outset that we do not suppose this theory to be a "correct" representation of the real situation, but only that it provides a convenient approximation which accounts for the transition and is probably as good as the current state of data measurement warrants.

Following Valley, then, we write

$$\sigma_x \equiv \sqrt{H(x)}\ \sigma_T \tag{47a}$$

and

$$\sigma_y \equiv \sqrt{1 - H(x)}\ \sigma_T \tag{47b}$$

where

$$H(x) \equiv x f(x) \tag{48}$$

and

$$f(x) \equiv \int_0^\infty \frac{\sin t}{t + x}\, dt \tag{49}$$

This function $f(x)$ is related to the Sine and Cosine Integrals, and its properties are discussed in Sec. 5.2 of the Handbook of Mathematical Functions.[18]

Finally, using these values of P, σ_x, σ_y, we compute the normalized output amplitude R and thence the output fundamental parameter γ. If we can ignore the time correlation of successive samples, this is easily done as follows: select random numbers S_x and S_y from zero-mean Gaussian distributions with variances σ_x^2 and σ_y^2, respectively. Then compute

$$R^2 = (P + S_x)^2 + S_y^2 \tag{50}$$

and

$$\gamma = \frac{\tau BR^2}{2} \tag{51}$$

In order to include the effects of time correlation, we proceed as previously described for the correlated phase samples **(page 23)**. The first samples, S_{x1}, S_{y1}, are selected as above. Succeeding samples, S_{xn}, S_{yn}, are computed from the formula

$$S_{xn} = FS_{x(n-1)} + \sqrt{1 - F^2}\, S'_x \tag{52}$$

where S'_x = the new sample from the Gaussian distribution

$S_{x(n-1)}$ = the prior computed value

and

$$F \equiv \exp(-\Delta t/\tau_D)$$

and its counterpart for S_{yn}.

7 INPUTS

The satellite communications model can be run by setting up the proper FLEXRED "tree" structure in the input stream. The user starts by putting a communication event dataset on the event list, and then satisfies the data input requirements that emanate from this dataset by inputting five further datasets: (1) the uplink dataset, which defines the parameters for the uplink transmitter-receiver pair; (2) the downlink dataset, which contains similar parameters for the downlink; (3) the transmitter platform dataset, which gives the position of the ground transmitter; (4) the satellite platform dataset, which gives the satellite's starting position and orbital parameters (if appropriate); and (5) the receiver platform dataset, which gives the position of the ground receiver. The contents of these datasets are defined in detail in Appendix A.

An example data deck for the communication model was set up to test the code. It was generated by modifying the nominal HIGHALT data deck described in Volume 1. The listing beginning on the next page shows the set of UPDATE change directives used on the ROSCOE DATDEK file to produce the example input deck.

Card 4 introduces a new scale factor for converting inputs in watts to the internally used ergs/second. Cards 6-8 are flags for diagnostic output in the new communications event overlays, and cards 10-12 denote overlay number as a function of event number.

The changes included in cards 13-32 establish the communications outputs and their formats, discussed in Sec. 8. Card 34 is a dataset pointer to the communications event, which places the first communications event on the input event list. Subsequent communications events will be generated by the program, using the time step in the communications event dataset (Card 44).

Cards 37-122 contain the input parameter datasets used by the communication routines. Cards 37-56 constitute the communications event dataset, 57-81 the uplink dataset, 82-106 the downlink dataset, 108-110 the ground transmitter platform dataset, 111-113 the ground receiver platform dataset, and 114-120 the satellite platform dataset. We will discuss these in turn. Card 122 gives the simulation stop time.

```
DATA DECK MODS FOR SAMPLE COMMUNICATIONS CASE

  1     *IDENT CMODSM
  2     *COMPILE MIGHALT
  3     *I MIGHALT,30
  4     WATTS TO ERGS/SEC                          WATTS     10000000.           SCALE
  5     *I MIGHALT,74
  6     EVENT 22 OUTPUT                            NO
  7     EVENT 23 OUTPUT                            NO
  8     EVENT 24 OUTPUT                            NO
  9     *I MIGHALT,97
 10     EVENT 22 CALLS OVERLAY                     22.0      INT
 11     EVENT 23 CALLS OVERLAY                     23.0      INT
 12     EVENT 24 CALLS OVERLAY                     24.0      INT
 13     *I MIGHALT,114
 14     OC OUTPUT LIST                             1.0                           ZEROS
 15     *I MIGHALT,122
 16     OC OUTPUT FORMAT LIST                                                    REFER
 17     *I MIGHALT,150
 18     OC OUTPUT FORMAT LIST                                                    BEG LIST
 19     OC OUTPUT FORMAT DATASET                                                 REFER
 20     *I MIGHALT,336
 21     OC OUTPUT FORMAT DATASET                                                 BEG SET
 22             TYPE OF OUTPUT                     OUTCCL
 23             COMMUNICATIONS OUTPUT                                            TITLE
 24             TYPE OF OUTPUT          01019        TYPE   OF OUTPUT           OUTCCL
 25             TIME OF OUTPUT          02020        TIME   OF OUTPUT SEC       OUTCCL
 26             UPLINK LOSS FACTOR      04034      UPLINK     LOSS     FACTOR   OUTCCL
 27             UPLINK SCINT.           07041      UPLINK     SCINT             OUTCCL
 28             DOWNLINK LOSS FACTOR    09054    DOWNLINK     LOSS     FACTOR   OUTCCL
 29             DOWNLINK SCINT.         12061    DOWNLINK     SCINT             OUTCCL
 30             PROB ERROR=SATELLITE    14071      PROB.    OF ERROR SATELLITE OUTCCL
 31             PROB ERROR=GROUND       15081      PROB.    OF ERROR    GROUND OUTCCL
 32             PROBABILITY OF ERROR    16091      PROB.    OF ERROR           OUTCCL
 33     *I MIGHALT,342
 34     COMMUNICATIONS EVENT DATASET                                             REFER
 35     *D MIGHALT,344,MIGHALT,345
 36     *I MIGHALT,346
 37     *   COMMUNICATIONS EVENT DATABETS                                        PRINT
 38     COMMUNICATIONS EVENT DATABET                                             BEG SET
 39             EVENT TYPE                         22.       INT
 40     EVENT TIME                                 1612.     SEC
 41             TRANSMITTER PLATFORM DATASET                                     REFER
 42             SATELLITE PLATFORM DATASET                                       REFER
 43             RECEIVER PLATFORM DATASET                                        REFER
 44     TIME STEP                                  10.       SEC
 45             TYPE OF MODULATION                 DPSK
 46             REGENERATION AT SATELLITE          YES
 47             COHERENT PSK MODULATION            NO
 48             FULLY DETERMINISTIC MODE           NO
 49             CONSTANT ZETA                      .707
 50             ORDER OF PHASE LOCKED LOOP         FIRST
```

```
51              UPLINK DATASET                                          REFER
52              DOWNLINK DATASET                                        REFER
53      SPACE FOR INTERNAL CALCULATIONS         0.0                     ZEROB
54      INITIAL VALUE FOR T1                    -10.    SEC
55      INITIAL VALUE FOR T2                    -10.    SEC
56      SPACE FOR INTERNAL CALCULATIONS         9.                      ZEROB
57              UPLINK DATASET                                          BEG SET
58      POWER                                   100.    WATTS
59      FREQUENCY                               8000.   MHZ
60      TRANSMITTER GAIN                        61.     DB
61      RECEIVER GAIN                           16.8    DB
62      TRANSMITTER LOSS FACTOR                 2.5     DB
63      SYSTEM LINE LOSS FACTOR                 0.5     DB
64              PHASED ARRAY TRANSMITTER        NO
65              UPLINK XMTR AZIM ERROR          0.      DEG
66              UPLINK XMTR ELEV ERROR          0.      DEG
67      SPACE FOR BORESIGHT VECTOR              3.                      ZEROS
68              PHASED ARRAY RECEIVER           NO
69              UPLINK RCVR AZIM ERROR          0.      DEG
70              UPLINK RCVR ELEV ERROR          0.      DEG
71      SPACE FOR BORESIGHT VECTOR              3.                      ZEROS
72      BIT PERIOD FOR UPLINK                   1.0E-8
73      IF FILTER BANDWIDTH                     125.    MHZ
74      BANDWIDTH FOR PLL                       125.    MHZ
75      BEAMWIDTH                               1.5     DEG
76      SIGNAL-TO-NOISE THRESHOLD               15.     DB
77      SIDELOBE LEVEL                          30.     DB
78              SPACE FOR BIT ERROR,PHASE ERROR2.0                      ZEROB
79              RECEIVER NOISE TEMPERATURE      720.
80              SPACE FOR NOISE FIGURE,TEMP     2.0                     ZEROB
81      SPACES FOR INTERNAL CALCULATIONS        32.                     ZEROB
82              DOWNLINK DATASET                                        BEG SET
83      POWER                                   20.     WATTS
84      FREQUENCY                               7400.   MHZ
85      TRANSMITTER GAIN                        33.2    DB
86      RECEIVER GAIN                           61.     DB
87      TRANSMITTER LOSS FACTOR                 3.2     DB
88      SYSTEM LOSS FACTOR                      0.5     DB
89              PHASE ARRAY TRANSMITTER         NO
90              DNLINK XMTR AZIM ERROR          0.      DEG
91              DNLINK XMTR ELEV ERROR          0.      DEG
92      SPACE FOR BORESIGHT VECTOR              3.                      ZEROS
93              PHASED ARRAY RECEIVER           NO
94              DNLINK RCVR AZIM ERROR          0.      DEG
95              DNLINK RCVR ELEV ERROR          0.      DEG
96      SPACE FOR BORESIGHT VECTOR              3.                      ZEROS
97      BIT PERIOD FOR DOWNLINK                 1.0E-8
98      IF FILTER BANDWIDTH                     125.    MHZ
99      BANDWIDTH FOR PLL                       125.    MHZ
100     BEAMWIDTH                               1.5     DEG
101     SIGNAL-TO-NOISE THRESHOLD               15.     DB
102     SIDELOBE LEVEL                          30.     DB
103             SPACE FOR BIT ERROR,PHASE ERROR2.0                      ZEROS
104     RECEIVER NOISE TEMPERATURE              200.
105             SPACE FOR NOISE FIGURE,TEMP     2.0                     ZEROS
106     SPACE FOR INTERNAL CALCULATIONS         32.                     ZEROS
107     *   TRANSMITTER, RECEIVER, AND SATELLITE POSITIONS              PRINT
108             TRANSMITTER PLATFORM DATASET                            BEG SET
109             TYPE OF PLATFORM                FIXED
110             POSITION                        0.0     -79.33  47.75   GEOGR
111             RECEIVER PLATFORM DATASET                               BEG SET
112             TYPE OF PLATFORM                FIXED
113             POSITION                        0.0     -83.    42.5    GEOGR
114             SATELLITE PLATFORM DATASET                              BEG SET
115             TYPE OF PLATFORM                CIRCULAR
116             INCLINATION                     90.     DEG
117             LONGITUDE                       -79.33  DEG
118             ARG. OF POINT-OF-INTEREST       47.75   DEG
119             TIME AT POINT-OF-INTEREST       1660.   SEC
120             PERIOD                          6650.   SEC
121     *  HIGHALT,365
122             STOP TIME                       1721.   SEC
```

Communications Event Dataset (Cards 37-56)

39	Event type (always 22 with current model)
40	Event time for first communication event
41-43	Pointers to ground transmitter, satellite, and ground receiver platform datasets
44	Time step between subsequent communication events
45	Modulation type (CPSK for coherent phase shift keying, DPSK for differential phase shift keying, or FSK for frequency shift keying)
46	Regeneration flag (YES for signal regeneration at satellite, NO if not)
47	Coherent FSK flag (YES for coherent FSK modulation, NO otherwise)
48	Fully deterministic mode flag (YES for fully deterministic simulation, NO otherwise--see Section 6)
49	Constant zeta (a constant used in the second-order PLL mode, currently set to 0.707)
50	Order of PLL (FIRST for first-order phase-locked loop, SECOND for second-order)
51-52	Pointers to the uplink and downlink datasets
53	Space for six variables computed internally (input 6.0 zeros)
54	Initial value of T1* (set to -10 on input for initialization)
55	Initial value of T2 (set to -10)
56	Space for nine internal variables (input 9.0 zeros)

Uplink Dataset (Cards 57-81)

58	Transmitter power
59	Transmitter frequency
60	Transmitter gain
61	Receiver gain
62	Transmitter loss factor (between transmitter and its antenna)

*T1 and T2 are used internally for keeping track of the times at which data samples are taken (for time correlation purposes).

63	System line loss between satellite antenna and satellite transponder's IF amplifier
64	Phased array transmitter flag (YES for phased array, NO otherwise)
65-66	Azimuth and elevation pointing errors of transmitter antenna
67	Space for transmitter antenna boresight (enter 3.0 zeros)
68	Phased array receiver flag (YES for phased array, NO otherwise)
69-70	Azimuth and elevation pointing errors of receiver antenna
71	Space for receiver antenna boresight (enter 3.0 zeros)
72	Bit period for uplink
73	IF filter bandwidth
74	Bandwidth for phase locked loop
75	Beamwidth of transmitter antenna
76	Signal-to-noise threshold for accepting signals
77	Receiver sidelobe level
78	Space for bit error and phase error computed internally (input 2.0 zeros)
79	Receiver noise temperature (enter value here or enter noise figure and physical temperature of receiver in the next two words)
80	Spaces for noise figure and physical temperature (enter 2.0 zeros if noise temperature is input above)
81	Spaces for internal calculations (enter 32.0 zeros)

Downlink Dataset (Cards 82-106)

Same type of data as for the uplink dataset

Transmitter Platform Dataset (Cards 108-110)

109	Type of platform (enter FIXED for a platform fixed with respect to the earth. Other options are CIRCULAR for circular orbits, ORBITAL or ELLIPTICAL for elliptic orbits)
110	Position of the fixed platform (Note: other types require additional inputs (see descriptions of datasets P1, P2, P3, and P4 in Appendix A)

Receiver Platform Dataset (Cards 111-113)

112	Type of platform
113	Position of the fixed platform

Satellite Platform Dataset (Cards 114-120)

115	Type of platform (CIRCULAR orbit)
116	Orbital inclination
117	Longitude of satellite's ascending node at time of arrival at reference point-of-interest
118	Earth-centered angular travel of satellite past its ascending node at reference point-of-interest
119	Time of arrival of satellite at reference point-of-interest
120	Orbital period of satellite

8 OUTPUTS

A single output table has been constructed to display the communication results. The OUTCOL format described in Volume I of this manual is used; it sets up a maximum of ten column headings and displays any variables the user specifies, in the format defined in the input deck.

For the communication model these outputs are given:

Column 1 — Type of Output. Program prints the message COM-RECEVD if the communications are received, or UP-LIMITED or DN-LIMITED if the signal noise drops below a specified threshold in either the uplink or downlink direction.

Column 2 — Time of Output. The engagement time for this line of output.

Column 3 — Uplink Loss Factor. Uplink propagation loss factor (dB)

Column 4 — Uplink Scintillation. Standard deviation of phase scintillations affecting uplink (rad)

Column 5 — Downlink Loss Factor. Downlink propagation loss factor (dB)

Column 6 — Downlink Scintillation. Standard deviation of phase scintillations affecting downlink (rad)

Column 7 — Probability of Error Satellite. Probability of element error in received signal demodulated at the satellite (for regenerative systems only)

Column 8 — Probability of Error Ground. Probability of element error in received signal demodulated at the ground after regeneration at the satellite

Column 9 — Probability of Error. Probability of element error in received signal

The output produced by running the HIGHALT data deck (Vol. 1) with the modifications described in the preceding section is shown on the next page. The simulation starts at a time 1612 seconds with the first communications event. A large burst goes off at 1620 seconds, directly above the transmitter. Forty seconds later, the satellite passes over the transmitter.

The communication outputs show that the burst disrupts the uplink signal for about 20-30 seconds because of severe absorption. Later scintillation effects cause continued severe degradation of communication reliability.

COMMUNICATIONS OUTPUT

TYPE OF OUTPUT	TIME OF OUTPUT SEC	UPLINK LOSS FACTOR	UPLINK SCINT	DOWNLINK LOSS FACTOR	DOWNLINK SCINT	PROB. OF ERROR SATELLITE	PROB. OF ERROR GROUND	PROB. OF ERROR
COMMRECEVD	1612.000	1.001	0.	1.605	0.	0.	0.	0.
UPLIMITED	1622.000	**********	.15246E+08	0.000	0.	.50000	.50000	.50000
UPLIMITED	1632.000	**********	.99177E+07	0.000	0.	.50000	.50000	.50000
COMMRECEVD	1642.000	41.841	.30454E+06	1.605	.17919E-04	.49896	0.	.49896
COMMRECEVD	1652.000	1.825	46801.	1.613	466.52	.23744	.87895E-17	.23744
COMMRECEVD	1662.000	1.241	65493.	1.659	11099.	.39805	.49802	.49960
COMMRECEVD	1672.000	1.283	.18955E+06	1.694	28181.	.49911	.29279	.49963
COMMRECEVD	1682.000	1.604	.70896E+06	1.703	74330.	.49589	.11933	.49687
COMMRECEVD	1692.000	1.121	.15559E+06	1.718	.11024E+06	.46409	.16215	.47573
COMMRECEVD	1702.000	1.094	.12131E+06	1.725	.11363E+06	.92345E-01	.42329	.43746
COMMRECEVD	1712.000	1.099	.45690E+06	1.732	.11238E+06	.45308	.82870E-01	.46086

REFERENCES

1. Schwartz, Bennett, and Stein, Communication Systems and Techniques, McGraw-Hill (1966), Chapter 7.

2. J.R. Garbarino, The ROSCOE Manual, Vol. 1, "Program Description," General Research Corporation CR-1-520, August 1975.

3. J. Marshall and P. Hu, A Computer Code for the Prediction of Satellite Communication System Performance in a Nuclear Environment (SATL) (U), ESL, Inc., ESL-TM241, 1 March 1972, Sec. 4.

4. D.C. Hogg and W.W. Mumford, "The Effective Noise Temperature of the Sky," Microwave Journal, 3, March 1960, pp. 80-84.

5. J. Roberts, et al., PSK Satellite Communication Systems in a Nuclear Environment (U), ESL Incorporated ESL-TM391 (DNA 3289T), 26 October 1973 (CONFIDENTIAL).

6. V. Mower, et al., Noncoherent PSK Satellite Communication Systems in a Nuclear Environment (U), ESL Incorporated ESL-TM504 (DNA 3529T), 6 September 1974 (SECRET FORMERLY RESTRICTED DATA).

7. Reference 1, Appendix A.

8. A.J. Viterbi, Principles of Coherent Communication, McGraw-Hill (1966), Chapter 2.

9. W.C. Lindsey, "Phase-Shift-Keyed Signal Detection With Noisy Reference Signals," IEEE Transactions on Aerospace and Electronic Systems, 2, July 1966, pp. 393-401.

10. Reference 1, p. 304.

11. R.P. Mercier, "Diffraction by a Screen Causing Large Random Phase Fluctuations," Proc. Camb. Phil. Soc., 58, pp. 383-400 (1962).

12. B.H. Briggs and I.A. Parkin, "On the Variation of Radio Star and Satellite Scintillations With Zenith Angle," J. Atmos. & Terr. Phys., 25, pp. 339-365 (1963).

13. R.S. Lawrence, C.G. Little, and H.J.H. Chivers, "A Survey of Ionospheric Effects Upon Earth-Space Radio Propagation," Proc. IEEE, 52, pp. 4-27 (1964).

REFERENCES (Cont.)

14. D.G. Singleton, "Saturation and Focusing Effects in Radio-Star and Satellite Scintillations," J. Atmos. and Terr. Phys., 32, pp. 187-208 (1970).

15. C.L. Rino and E.J. Fremouw, "Statistics for Ionospherically Diffracted VHF/UHF Signals," Radio Science, 8, pp. 223-233 (1973).

16. G.C. Valley, "The Relation Between the Specular to Interference Ratio and the Scintillation Index," IEEE Trans. Comm., COM-23, pp. 1351-1354 (1975).

17. S.O. Rice, "Mathematical Analysis of Random Noise," Bell System Tech. J., 23, 282-332 (July 1944), and 24, 46-156 (January 1945); [esp. Sec. 3.10].

18. M. Abramowitz and I.A. Stegun (Ed.), Handbook of Mathematical Functions, Dover Publications (1965).

APPENDIX A

COMMUNICATIONS DATASETS

The following pages contain the "DSCRIP" cards for datasets which are of direct use for communications cases. DSCRIP cards are discussed in Vol. 3 of this manual. The C3, CU, CD, OC, and P4 datasets are new, having been added to the basic ROSCOE DSCRIP file for the communications version of the code. The P1, P2, and P3 datasets are not new; they are included here only because they represent alternate modes of platform input for communications cases.

DESCRIPTION OF DATASETS USED IN COMMUNICATIONS CASES

```
*/ ------------------------------------------------------------------
*/
*/       C3 DATASET (COMMUNICATIONS EVENT)
*/
*/ ------------------------------------------------------------------
NEW C3          COMMUNICATIONS EVENT DATASET
I   KTYPE       EVENT TYPE (=22)
R   TIME        TIME OF THIS EVENT
DSP PLATT       POINTER TO TRANSMITTER PLATFORM DATASET
DSP PLATS       POINTER TO SATELLITE PLATFORM DATASET
DSP PLATR       POINTER TO RECEIVER PLATFORM DATASET
R   TSTEP       TIME STEP FOR COMMUNICATION EVENTS
H   TYPE        ENTER--CPSK,DPSK,FSK--FOR COMMUNICATIONS TYPE
H   REGEN       FLAG--YES--FOR REGENERATION AT SATELLITE
H   COH         FLAG--YES--FOR PSK COHERENT MODE
H   DET         FLAG--YES--FOR FULLY DETERMINISTIC MODE
R   ZETA        A CONSTANT
H   PLL         ENTER--FIRST,SECOND--FOR ORDER OF PHASE LOCKED LOOP
DSP DSPCU       POINTER TO UPLINK DATASET
DSP DSPCD       POINTER TO DOWNLINK DATASET
DSP DSPOC       POINTER TO OUTPUT DATASET
I   IFLAG       EVENT FLAG (SET =0 INITIALLY)
R4  CTH         OFF-AXIS BORESIGHT ANGLES
R   T1          STORED MEASUREMENT TIME
R   T2          LAST MEASUREMENT TIME
R   PHIU        UPLINK PHASE AT LAST MEASUREMENT TIME
R   PHID        DOWNLINK PHASE AT LAST MEASUREMENT TIME
R   PHIT        TOTAL PATH PHASE AT LAST MEASUREMENT TIME
R   SXU         UPLINK SIGMA IN X AT LAST TIME
R   SYU         UPLINK SIGMA IN Y AT LAST TIME
R   SXD         DOWNLINK SIGMA IN X AT LAST TIME
R   SYD         DOWNLINK SIGMA IN Y AT LAST TIME
R   TNEW1       NEW (MEASUREMENT = 1) TIME
R   TNEW2       NEW (MEASUREMENT = 2) TIME
*/
*/
*/ ------------------------------------------------------------------
*/
*/       CU DATASET (UPLINK DATASET)
*/
*/ ------------------------------------------------------------------
NEW CU          COMMUNICATIONS UPLINK DATASET
R   POWER       TRANSMITTED POWER
R   FREQ        FREQUENCY
R   GT          ON-AXIS GAIN OF TRANSMITTER
R   GR          ON-AXIS GAIN OF RECEIVER
R   XLU1        TRANSMITTER LOSS FACTOR
R   XLU2        SYSTEM (LINE) LOSS BETWEEN SATELLITE ANTENNA AND AMPLIFIER
H   ARRAT       ENTER--YES--FOR PHASED ARRAY TRANSMITTER
R   TAZER       TRANSMITTER BORESIGHT AZIMUTH ERROR
```

DESCRIPTION OF DATASETS USED IN COMMUNICATIONS CASES

```
R    TELER      TRANSMITTER BORESIGHT ELEVATION ERROR
R3   BVECT      BORESIGHT VECTOR OF TRANSMITTER
H    ARRAR      ENTER--YES--FOR PHASED ARRAY RECEIVER
R    RAZER      RECEIVER BORESIGHT AZIMUTH ERROR
R    RELER      RECEIVER BORESIGHT ELEVATION ERROR
R3   BVECR      BORESIGHT VECTOR OF RECEIVER
R    TAUU       BIT PERIOD FOR UPLINK
R    BU         IF FILTER BANDWIDTH OF SATELLITE RECEIVER
R    BLS        NOISE BANDWIDTH OF SATELLITE RECEIVER (PLL MODE)
R    BEAMR      RECEIVER BEAMWIDTH
R    SN         SIGNAL-TO-NOISE THRESHOLD
R    SL         SIDELOBE LEVEL
R    P0         DESIRED BIT ERROR RATE AT SATELLITE IF REGENERATION USED
R    SIGNS      RMS PHASE ERROR DUE TO NOISE IN THE SATELLITE
R               (ENTER EITHER BLS OR P0 AND SIGNS)
R    TRS        RECEIVER NOISE TEMPERATURE
R    NFS        RECEIVER NOISE FIGURE
R    TPS        PHYSICAL TEMPERATURE OF SATELLITE
R               (ENTER EITHER TRS OR NFS, TPS OPTIONAL)
R    SOU        SIGANL PARAMETER FOR UPLINK
R    TNU        NOMINAL SYSTEM NOISE TEMPERATURE FOR UPLINK
R    R          RANGE TO SATELLITE
R3   XLOSU      UPLINK LINE OF SIGHT
R    GAMU       UPLINK SIGNAL PARAMETER
R3   POS        POSITION OF TRANSMITTER
R10  STATT      TRANSMITTER STATE(GROUND)
R10  STATR      RECEIVER STATE(SATELLITE)
R    XU         UPLINK BANDWIDTH /TIME PRODUCT
R    XLFU       UPLINK MISMATCH LOSS FACTOR
*/
*/
*/ ------------------------------------------------------------------
*/
*/      CD DATASET (DOWNLINK DATASET)
*/
*/ ------------------------------------------------------------------
NEW  CD         COMMUNICATIONS DOWNLINK DATASET
R    POWER      TRANSMITTED POWER
R    FREQ       FREQUENCY
R    GT         ON-AXIS GAIN OF TRANSMITTER
R    GR         ON-AXIS GAIN OF RECEIVER
R    XLD1       TRANSMITTER LOSS FACTOR
R    XLD2       SYSTEM LOSS ON GROUND
H    ARRAT      ENTER-- YES-- FOR PHASED ARRAY TRANSMITTER
R    TAZER      TRANSMITTER BORESIGHT AZIMUTH ERROR
R    TELER      TRANSMITTER BORESIGHT ELEVATION ERROR
R3   BVECT      BORESIGHT VECTOR OF TRANSMITTER
H    ARRAR      ENTER--YES--FOR PHASED ARRAY RECEIVER
R    RAZER      RECEIVER BORESIGHT AZIMUTH ERROR
R    RELER      RECEIVER BORESIGHT ELEVATION ERROR
```

```
DESCRIPTION OF DATASETS USED IN COMMUNICATIONS CASES

                R3  BVECR       BORESIGHT VECTOR OF RECEIVER
                R   TAUD        BIT PERIOD FOR DOWNLINK
                R   BD          IF FILTER BANDWIDTH OF GROUND RECEIVER
                R   BLG         NOISE BANDWIDTH OF GROUND RECEIVER (PLL MODE)
                R   BEAMR       RECEIVER BEAMWIDTH
                R   SN          SIGNAL-TO-NOISE THRESHOLD
                R   SL          SIDELOBE LEVEL
                R   PO          DESIRED BIT ERROR RATE AT GROUND
                R   SIGR        RMS PHASE ERROR DUE TO NOISE IN THE GROUND RECEIVER
                P               (ENTER EITHER BLG OR PO AND SIGR)
                R   TRG         RECEIVER NOISE TEMPERATURE
                R   NFG         RECEIVER NOISE FIGURE
                R   TPG         PHYSICAL TEMPERATURE OF GROUND RECEIVER
                P               (ENTER EITHER TPG OR NFG, TPG OPTIONAL)
                R   SDD         SIGNAL PARAMETER FOR DOWNLINK
                R   TND         NOMINAL SYSTEM NOISE TEMPERATURE FOR DOWNLINK
                R   R           RANGE TO GROUND RECEIVER
                R3  XLOSD       DOWNLINK LINE OF SIGHT
                R   GAMD        DOWNLINK SIGNAL PARAMETER
                R3  POS         POSITION OF TRANSMITTER
                R10 STATT       TRANSMITTER STATE(SATELLITE)
                R10 STATR       RECEIVER STATE(GROUND)
                R   XD          DOWNLINK BANDWIDTH /TIME PRODUCT
                R   XLFD        DOWNLINK MISMATCH LOSS FACTOR
                */
                */
                */ ------------------------------------------------------------------
                */
                */      OC DATASET (OUTPUT DATASET FOR COMMUNICATIONS)
                */
                */ ------------------------------------------------------------------
                NEW OC          OUTPUT DATASET FOR COMMUNICATIONS
                M   TYPE        FLAG FOR MEASUREMENT TYPE (UP=LIMITED,DN=LIMITED,
                P               COM=RECEVD)
                R   TIME        TIME OF OUTPUT
                R   TN          UPLINK OR DOWNLINK SYSTEM TEMPERATURE
                R   XLPU        UPLINK PROPAGATION LOSS FACTOR
                R   XLDU        UPLINK DISPERSIVE LOSS FACTOR
                R   TAU         UPLINK ANTENNA NOISE TEMPERAURE
                R   XMU         DEVIATION OF PHASE SCINTILLATIONS IN UPLINK
                R   TDU         DECORRELATION TIME FOR SCINTILLATIONS IN UPLINK
                R   XLPD        DOWNLINK PROPAGATION LOSS FACTOR
                R   XLDD        DOWNLINK DISPERSIVE LOSS FACTOR
                R   TAD         DOWNLINK ANTENNA NOISE TEMPERATURE
                R   XMD         DEVIATION OF PHASE SCINTILLATIONS IN DOWNLINK
                R   TDD         DECORRELATION TIME FOR SCINTILLATIONS IN DOWNLINK
                R   PES         PROBABILITY OF ELEMENT ERROR IN SIGNAL AT SATELLITE
                R   PEG         PROBABILITY OF ELEMENT ERROR IN SIGNAL AT GROUND
                R   PE          PROBABILITY OF ELEMENT ERROR IN SIGNAL FOR TOTAL PATH
                R   XMT         DEVIATION OF PHASE SCINTILLATIONS FOR TOTAL PATH
```

DESCRIPTION OF DATASETS USED IN COMMUNICATIONS CASES

```
R    TDT        DECORRELATION TIME FOR SCINTILLATIONS FOR TOTAL PATH
*/
*/
*/ ------------------------------------------------------------------
*/
*/       P1 DATASET (FIXED PLATFORM)
*/
*/ ------------------------------------------------------------------
NEW P1          PLATFORM TYPE=1 (FIXED) DATASET
H    KTYPE      PLATFORM TYPE (ALWAYS =FIXED= FOR A FIXED PLATFORM
R3   POS        PLATFORM POSITION
*/
*/
*/ ------------------------------------------------------------------
*/
*/       P2 DATASET (ELLIPTIC ORBIT PLATFORM)
*/
*/ ------------------------------------------------------------------
NEW P2          PLATFORM TYPE 2 == TRAID ORBITAL ELEMENTS
H    KTYPE      PLATFORM MODEL TYPE ( = 7HORBITAL )
R10 ORBEL       A TRAID 10=VECTOR OF ORBITAL ELEMENTS
*/
*/
*/ ------------------------------------------------------------------
*/
*/       P3 DATASET (CIRCULAR ORBIT PLATFORM)
*/
*/ ------------------------------------------------------------------
NEW P3          PLATFORM TYPE 3 FOR CIRCULAR ORBITS
H    KTYPE      PLATFORM MODEL TYPE ( = 8HCIRCULAR )
R    AINC       INCLINATION OF ORBITAL PLANE
R    ALONG      LONGITUDE OF ASCENDING NODE (AS CALCULATED AT TIME BELOW)
R    OLOC       LOCATION IN ORBIT (AROUND FROM ASCENDING NODE)
R    TIME       TIME OF VALIDITY OF GIVEN DATA
R    PERI       PERIOD OF ORBIT
*/
*/
*/ ------------------------------------------------------------------
*/
*/       P4 DATASET (ORBITAL PLATFORM = CONVERTED TO P2 DATASET INTERNALLY)
*/
*/ ------------------------------------------------------------------
NEW P4          POSITION DATASET FOR SATELLITES (ELLIPTICAL ORBITS)
H    KTYPE      TYPE OF POSITION CALCULATION ( = ELLIPTICAL IN THIS CASE)
R    PERD       ORBITAL PERIOD OF SATELLITE
R    AINC       INCLINATION ANGLE OF ORBITAL PLANE
R    ASCN       LONGITUDE OF ASCENDING NODE (AT T = 0)
R    ARGP       ARGUMENT OF PERIGEE
R    PERAL      PERIGEE ALTITUDE
R    TMPER      TIME OF PERIGEE PASSAGE
```

APPENDIX B

MODIFICATIONS TO PROGRAM STRUCTURE

Development of the communications version of ROSCOE required modifications to nine routines: COLLF, EVPROC, FUZINC, OUTRTN, PLTFRM, POTSOL, REFRCT, REF1S, and ROSCOE. In addition, 27 new routines were added and three new overlays were required. Additional datasets were added; these are described in Appendix A. This appendix contains flow charts and definitions of symbols for the key routines of the communication model.

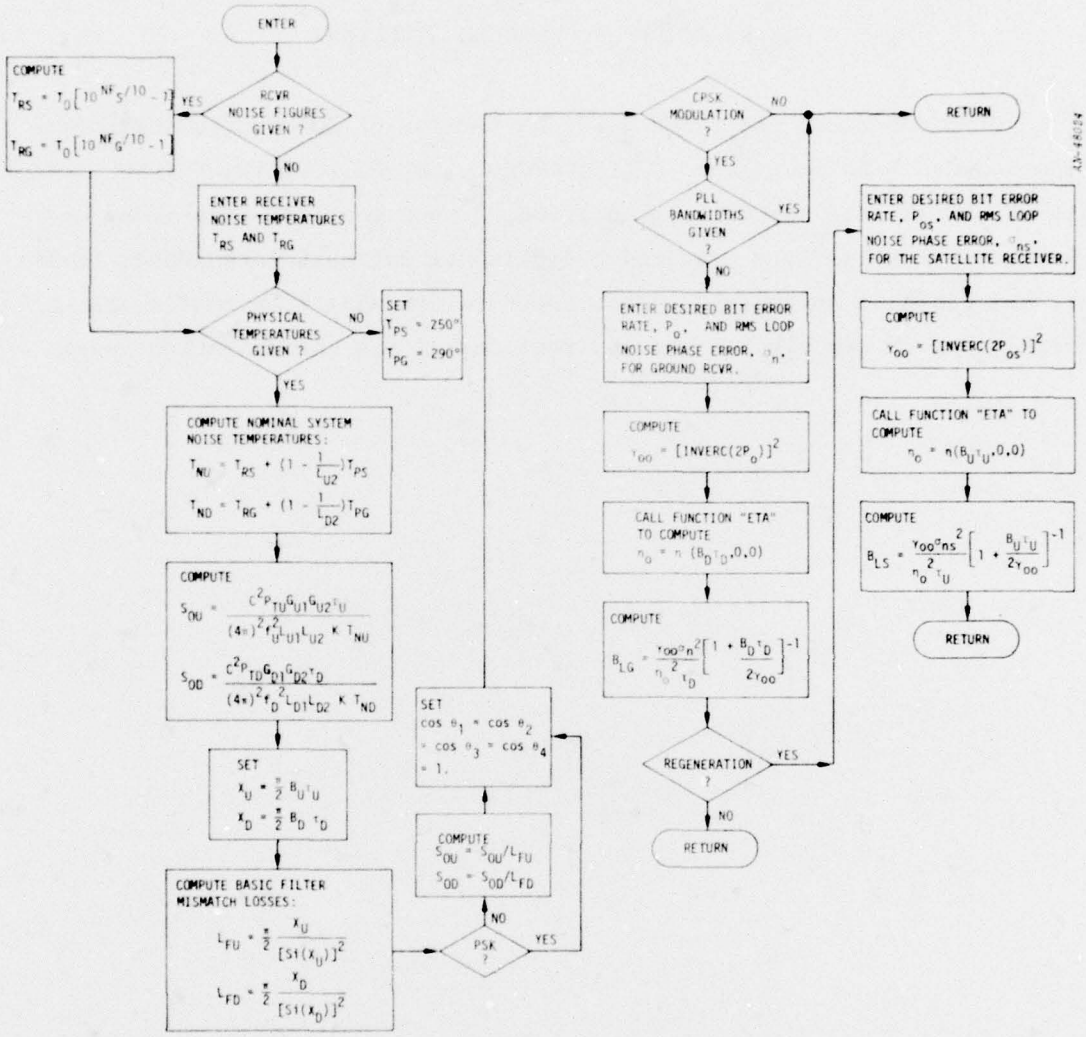

Figure B.1. Flow Diagram for Subroutine COMIN--Communication Initialization Routine

Definition of Symbols in Subroutine COMIN (Communications Initialization)

T_{RS}	Receiver noise temperature of satellite receiver, °K
T_{RG}	Receiver noise temperature of ground receiver, °K
T_o	Standard reference temperature = 290°K
$\overline{NF}_S$	Receiver noise figure for satellite receiver, dB
$\overline{NF}_G$	Receiver noise figure for ground receiver, dB
T_{PS}	Physical temperature of satellite receiver front end and transmission lines (default value = 250°K)
T_{PG}	Physical temperature of ground receiver front end and transmission lines (default value = 290°K)
T_{NU}	Nominal system noise temperature for uplink (satellite receiver)
T_{ND}	Nominal system noise temperature for downlink (ground receiver)
L_{U2}	System (line) loss between satellite receiving antenna and satellite transponder's IF amplifier
L_{D2}	System (line) loss between ground receiving antenna and ground receiver's IF amplifier
S_{OU}	Precomputable signal parameter for the uplink signal received at satellite
S_{OD}	Precomputable signal parameter for the downlink signal received at ground terminal
γ	"Gamma," a fundamental parameter for digital communications systems, defined as E_b/N_o, the ratio of total average received energy per signal element (bit) to noise power per unit bandwidth
C	Speed of light
P_{TU}	Total average radiated RF power at ground-terminal transmitting antenna

P_{TD}	Total average radiated RF power at satellite transmitting antenna (corrected for any "backoff" which may be required by a Frequency Division Multiple Access (FDMA) system to prevent serious intermodulation distortion)
G_{U1}	On-axis gain of ground transmitting antenna beam
G_{U2}	On-axis gain of satellite receiving antenna beam
G_{D1}	On-axis gain of satellite transmitting antenna beam
G_{D2}	On-axis gain of ground receiving antenna beam
τ_U	Bit period (element length) for uplink, s
τ_D	Bit period (element length) for downlink, s
f_U	Frequency of ground-transmitted (uplink) RF signal, Hz
f_D	Frequency of satellite-transmitted (downlink) RF signal, Hz
L_{U1}	System loss between ground transmitter and its antenna
L_{D1}	System loss between satellite transmitter and its antenna
K	Boltzmann's constant = 1.380622×10^{-23} J/°K
B_U	IF filter bandwidth of satellite receiver
B_D	If filter bandwidth of ground receiver
L_{FU}	Filter mismatch loss at satellite receiver, due to using a (rectangular) bandpass filter rather than a matched one
L_{FD}	Filter mismatch loss at ground receiver
Si(X)	Integral function $\int_0^X (\sin t)/t \, dt$
θ_J	Antenna pointing angle off boresight for antenna type J (initialized to zero here)

- $\theta_J \equiv 0$ always for steered dish antennas
- J = 1, ground transmitting antenna; J = 2, satellite receiving antenna; J = 3, satellite transmitting antenna; J = 4, ground receiving antenna

CPSK	"Coherent phase-shift keying" modulation
PLL	"Phase locked loop" used in demodulating a CPSK signal
P_o	Desired bit error rate for communication system, evaluated at the ground receiver
σ_n	RMS phase error due to noise in ground receiver's PLL, rad
γ_{oo}	"Gamma" (measured just prior to the receiver's demodulator in the absence of scintillations) required to produce bit error rate P_o for the CPSK system
η_o	Parameter computed by Function ETA, evaluated here in the absence of scintillations
B_{LG}	Noise bandwidth of ground receiver's PLL, Hz
P_{os}	Desired bit error rate at the satellite receiver if regeneration is being employed
σ_{ns}	RMS phase error due to noise in satellite receiver's PLL if regeneration is being employed, rad
B_{LS}	Noise bandwidth of satellite receiver's PLL if regeneration is being employed, Hz

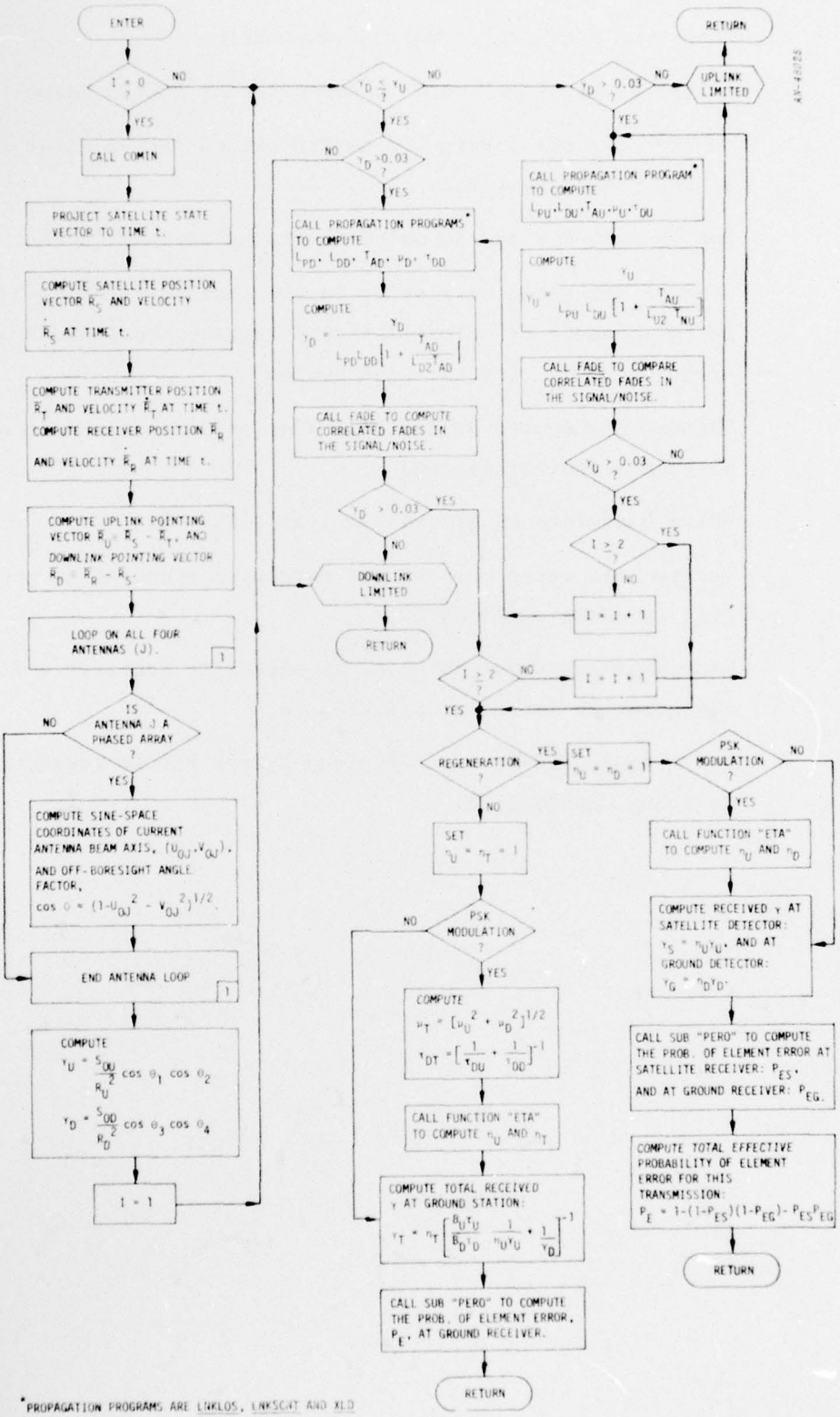

Figure B.2. Flow Diagram for Program COMLINK--Communications Event Program

Definition of Symbols in Program COMLINK

t	Simulated time of this communications event
$\bar{R}_S$	Position vector of satellite at time t
$\dot{\bar{R}}_S$	Velocity vector of satellite at time t
$\bar{R}_T$	Position vector of ground transmitting antenna at time t
$\dot{\bar{R}}_T$	Velocity vector of ground transmitting antenna at time t
$\bar{R}_R$	Position vector of ground receiving antenna at time t
$\dot{\bar{R}}_R$	Velocity vector of ground receiving antenna at time t
$\bar{R}_U$	Uplink pointing vector from ground transmitter to satellite at time t
$\bar{R}_D$	Downlink pointing vector from satellite to ground receiver at time t
J	Antenna designator: • $J = 1$, ground transmitting antenna; $J = 2$, satellite receiving antenna; $J = 3$, satellite transmitting antenna; $J = 4$, ground receiving antenna
U_{OJ}, V_{OJ}	Sine-space coordinates of current axis of antenna beam pattern for antenna J (= (0,0) for non-phased array antennas)
θ_J	See definitions for Subroutine COMIN
γ_U	Ratio of bit energy to noise power density for uplink
γ_D	Ratio of bit energy to noise power density for downlink
S_{OU}, S_{OD}	Precomputed constants; see definitions for Subroutine COMIN
R_U	Uplink range from ground transmitter to satellite = $\lvert\bar{R}_U\rvert$
R_D	Downlink range from satellite to ground receiver = $\lvert\bar{R}_D\rvert$
L_{PD}	Downlink propagation loss factor (ratio)
L_{DD}	Downlink dispersive loss factor (ratio)

T_{AD}	Downlink antenna noise temperature, °K (measured in ground receiving antenna)
μ_D	Standard deviation of phase scintillations affecting downlink, rad (assumed: zero-mean, Gaussian random phase process)
τ_{DD}	Decorrelation time for scintillations affecting downlink, s
L_{D2}	See definitions for Subroutine COMIN
L_{PU}	Uplink propagation loss factor (ratio)
L_{DU}	Uplink dispersive loss factor (ratio)
T_{AU}	Uplink antenna noise temperature, °K (measured in satellite receiving antenna)
μ_U	Standard deviation of phase scintillations affecting uplink, rad
τ_{DU}	Decorrelation time for scintillations affecting uplink, s
L_{U2}	See definitions for Subroutine COMIN
η_U	Parameter η (see below) computed for uplink path: $\eta(B_U\tau_U, \tau_U/\tau_{DU}, \mu_U)$
η_D	Parameter η (see below) computed for downlink path: $\eta(B_D\tau_D, \tau_D/\tau_{DD}, \mu_D)$
η_T	Parameter η (see below) computed for total path: $\eta(B_D\tau_D, \tau_D/\tau_{DT}, \mu_T)$
PSK	Phase-shift keying
μ_T	Standard deviation of phase scintillations affecting total path, rad
τ_{DT}	Decorrelation time for scintillations affecting total path, s
η	Fundamental factor relating to phase scintillations affecting PSK modulated signals; defined to be proportional to the integral of the power spectral density function of phase-distorted signal after passing through the IF filter

γ_T	Ratio of bit energy to noise power density for total path, computed just prior to ground receiver's detector
P_E	Probability of element error in received signal
γ_S	Ratio of bit energy to noise power density computed just prior to satellite receiver's detector (regenerative systems only)
γ_G	Ratio of bit energy to noise power density for downlink path, computed just prior to ground receiver's detector (regenerative systems only)
P_{ES}	Probability of element error in received signal demodulated at the satellite (regenerative systems only)
P_{EG}	Probability of element error in received signal demodulated at the ground after regeneration at the satellite

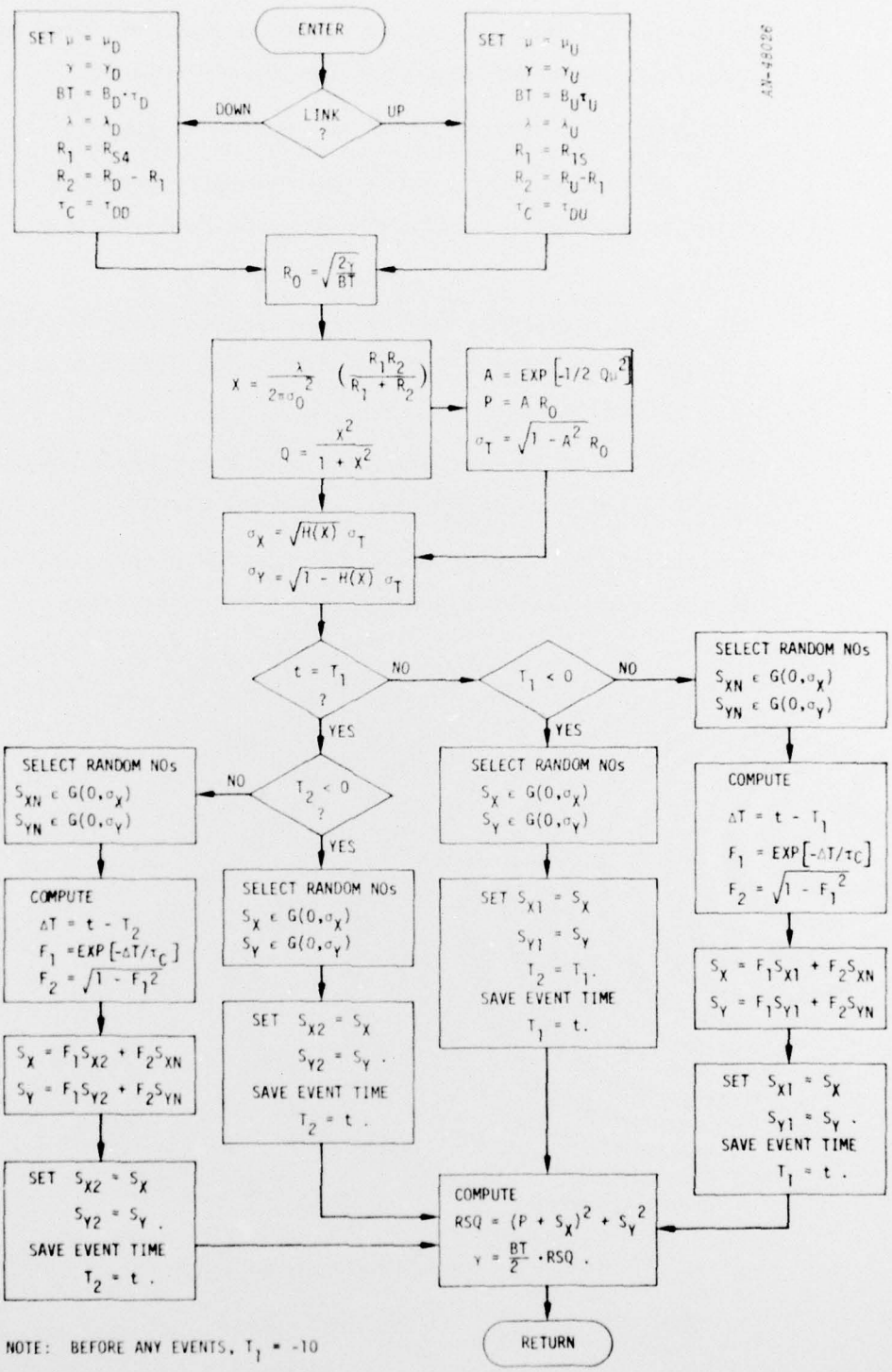

Figure B.3. Flow Diagram for Subroutine FADE--Computes Correlated Fades

Definition of Symbols in Subroutine FADE

μ	Standard deviation of phase scintillations affecting this link, rad
λ_U	Wavelength of uplink
λ_D	Wavelength of downlink
R_{1S}	Slant range from ground transmitting antenna to striated region
R_{S4}	Slant range from ground receiving antenna to striated region
R_U	Uplink range, from ground transmitting antenna to satellite
R_D	Downlink range, from satellite to ground receiving antenna
σ_0	Parameter appearing in striation size distribution; currently set equal to 1 km in a DATA statement
H(X)	Function HFUN (see subprogram flow diagram)
t	"time" of this event
$G(m,\sigma)$	Gaussian probability distribution; notation $S_X \varepsilon G(0,\sigma_X)$ means "draw a random number S_X from a zero-mean Gaussian distribution with standard deviation σ_X."
T_1	Stored measurement time for time correlation calculations
T_2	Last measurement time for time correlation calculations

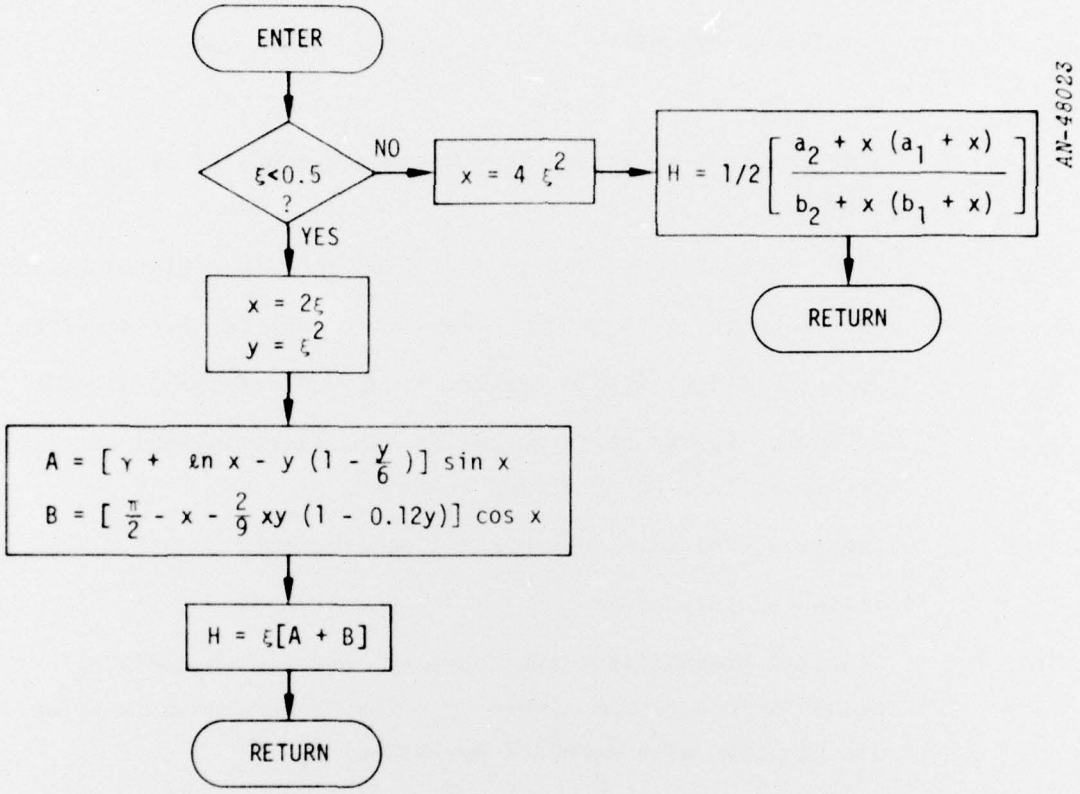

WHERE: $a_1 = 7.241163$ $a_2 = 2.463936$

$b_1 = 9.068580$ $b_2 = 7.157433$

$\gamma = 0.5772156649$

Figure B.4. Flow Diagram for Function HFUN

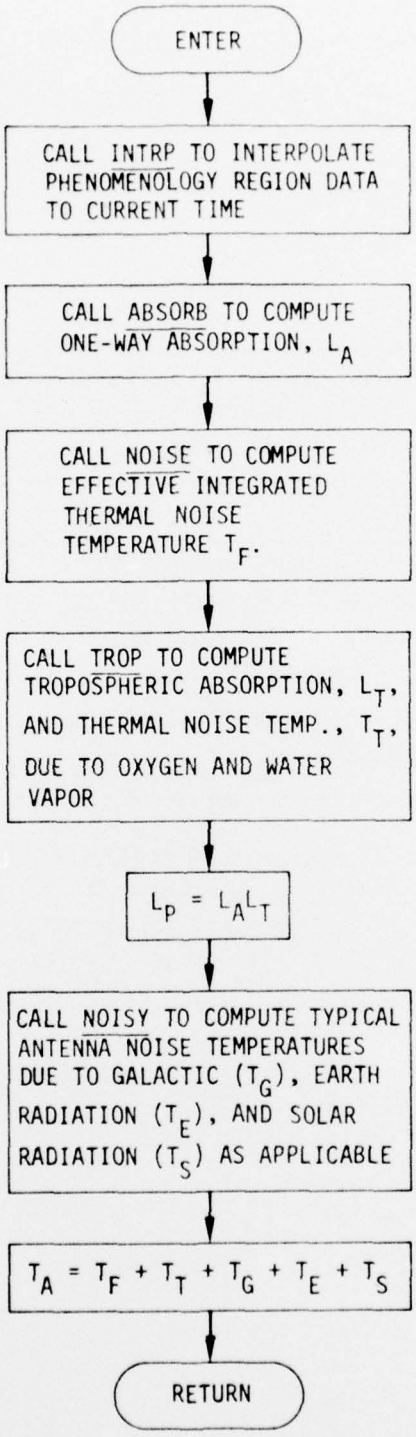

Figure B.5. Flow Diagram for Program LNKLOS--Computes Absorption and Noise Losses

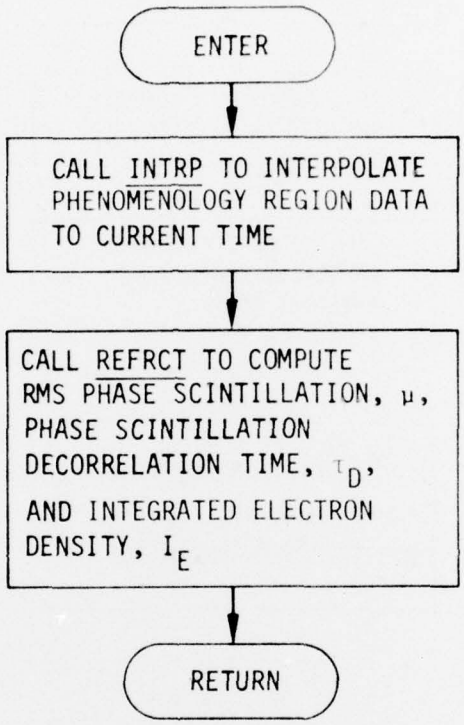

Figure B.6. Flow Diagram for Program LNKSCNT--Computes Scintillation Effects

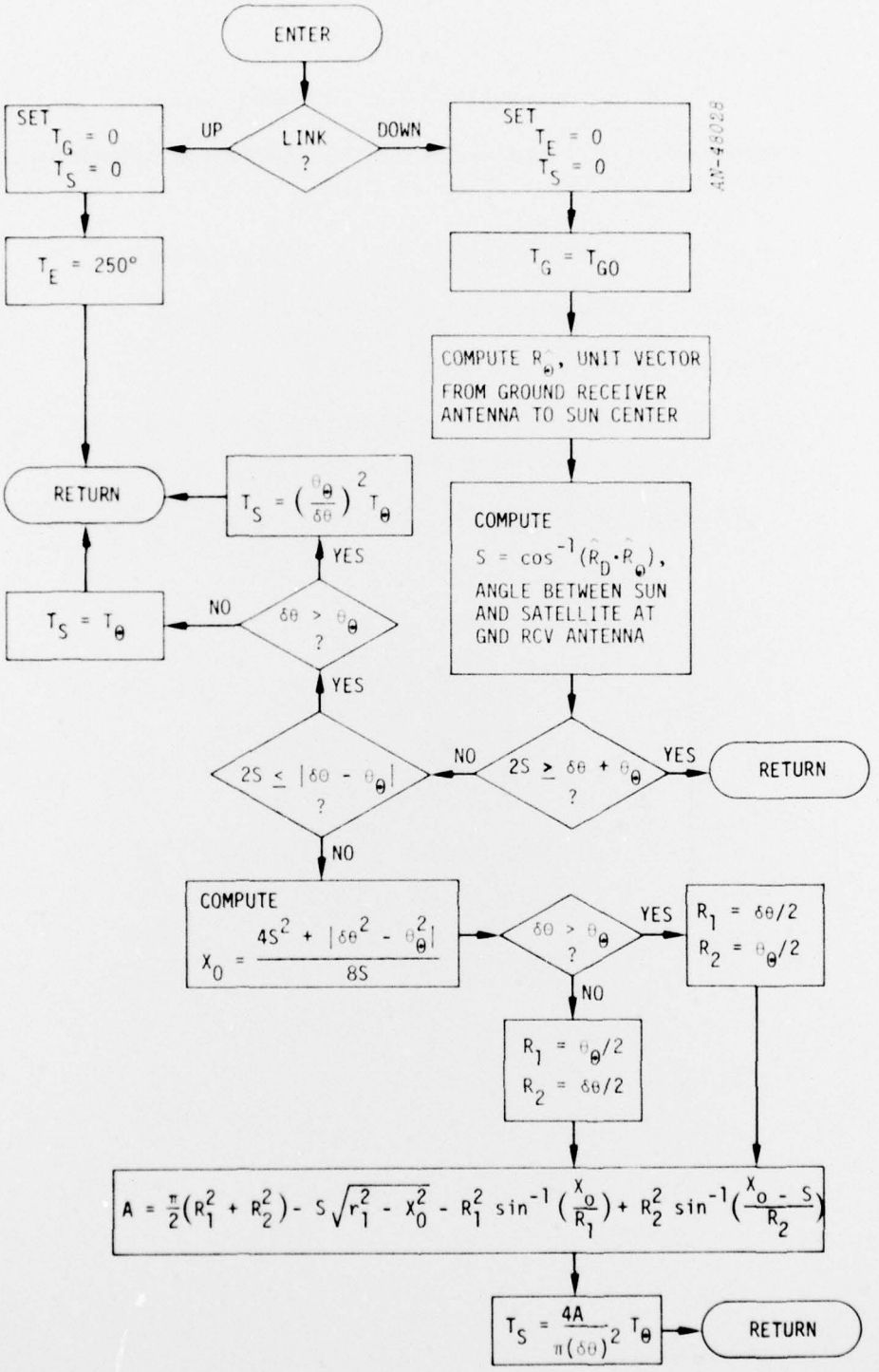

Figure B.7. Flow Diagram for Subroutine NOISY--Computes Antenna Noise Temperatures

Definition of Symbols for Subroutine NOISY

T_G Antenna noise temperature due to (mean) galactic sources, °K

T_E Antenna noise temperature due to **(estimated) earth radiation,** °K

T_S Antenna noise temperature due to solar radiation, °K

$\delta\theta$ Beamwidth of the ground receiving antenna

θ_Θ Angular diameter of the sun = 0.5°

T_{GO} Average galactic noise temperature, °K* $= 2.6 \times 10^{19}/f_D^2$ where f_D = downlink RF frequency, Hz

T_Θ Equivalent noise temperature of the quiet sun*

$$T_\Theta = \begin{cases} \dfrac{2.0 \times 10^{14}}{f_D} \\ \quad \text{if} \quad f_D < 2.5 \times 10^8 \quad \text{or} \quad f_D > 3.5 \times 10^{10} \ \text{Hz} \\ \dfrac{2.0 \times 10^{14}}{f_D}\left\{1 + \dfrac{1}{2.3}\sin 2\pi\left[\dfrac{\log_{10} 6(f_D \times 10^{-9} - 0.10)}{2.3}\right]\right\} \\ \quad \text{if} \quad 2.5 \times 10^8 \leq f_D \leq 3.5 \times 10^{10} \ \text{Hz} \end{cases}$$

*Precomputed during "initialization" and stored in a list.

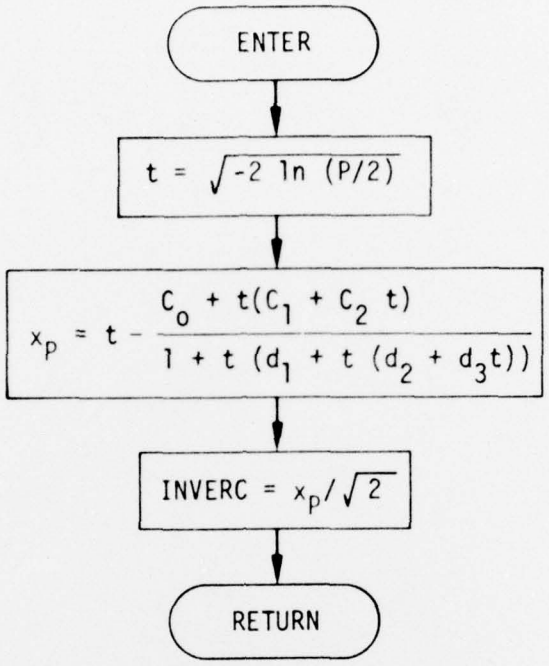

CONSTANTS

C_o	= 2.515517	d_1	= 1.432788
C_1	= 0.802853	d_2	= 0.189269
C_2	= 0.010328	d_3	= 0.001308

Source: Abramowitz & Stegun, 26.2.23.

Figure B.8. Flow Diagram for Function INVERC--Inverts the Error Function ERFC (Z)

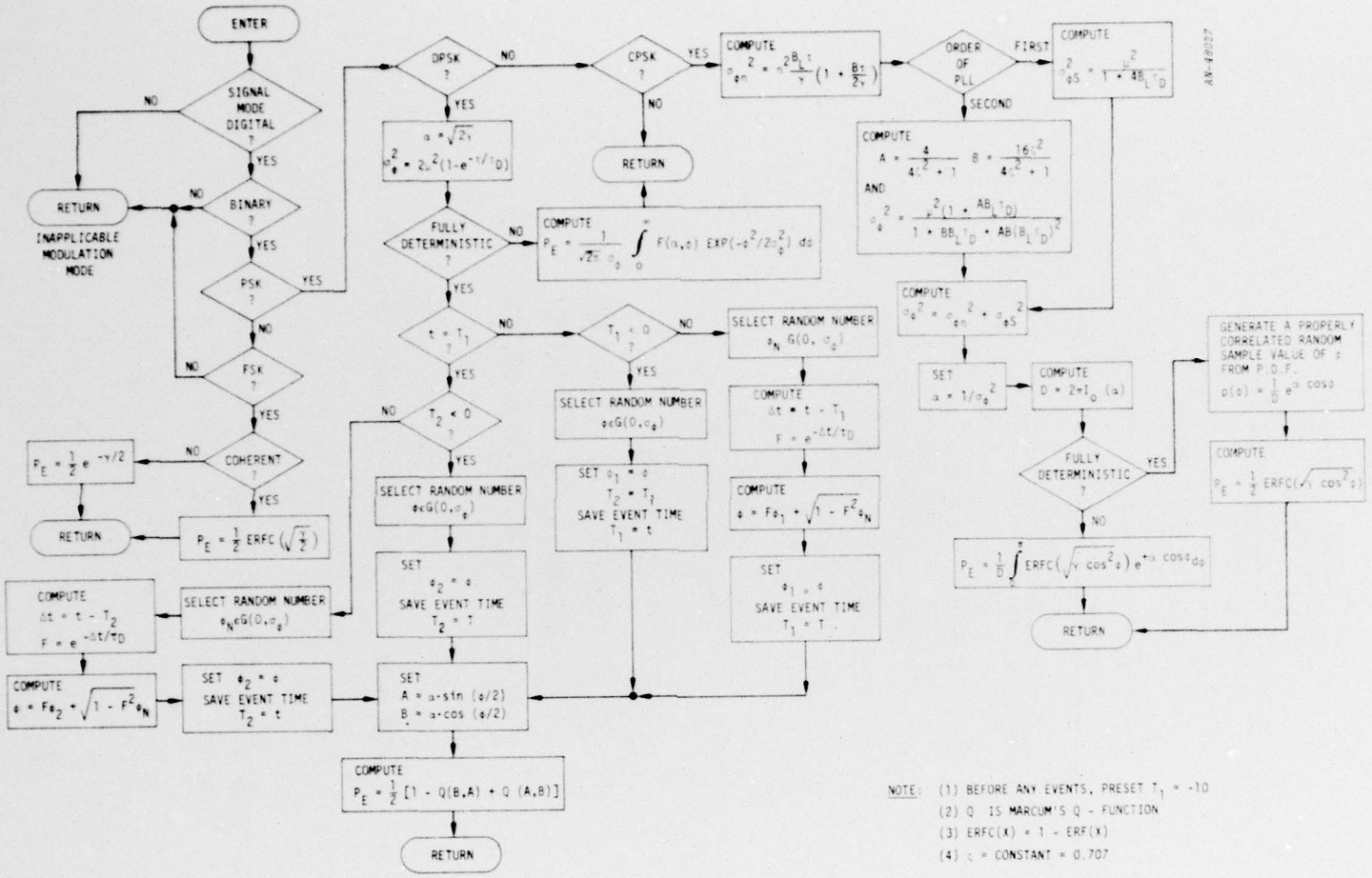

Figure B.9. Flow Diagram for Subroutine PERO--Computes Probability of Bit Error

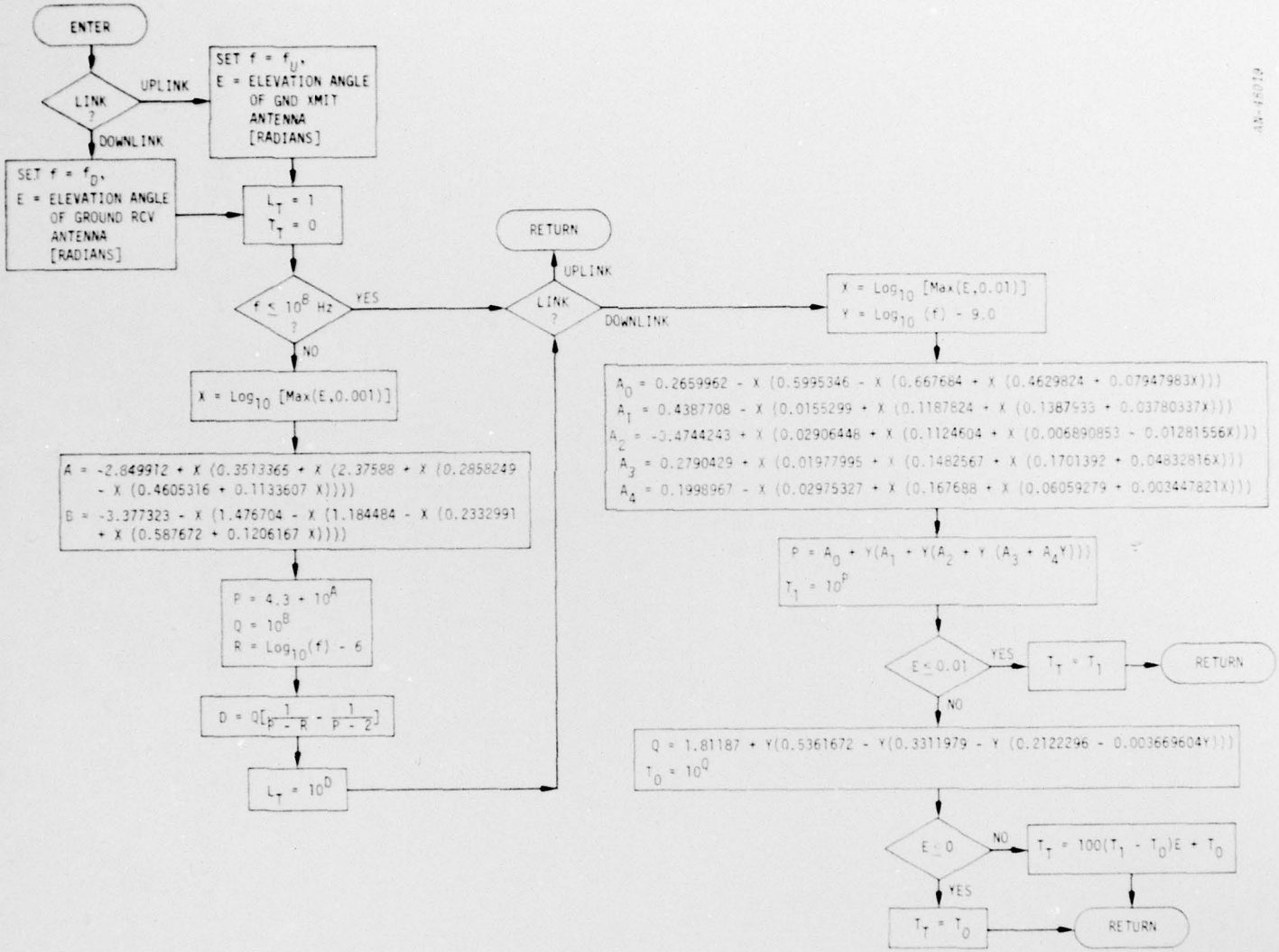

Figure B.10. Flow Diagram for Subroutine TROP--Computes Tropospheric Absorption

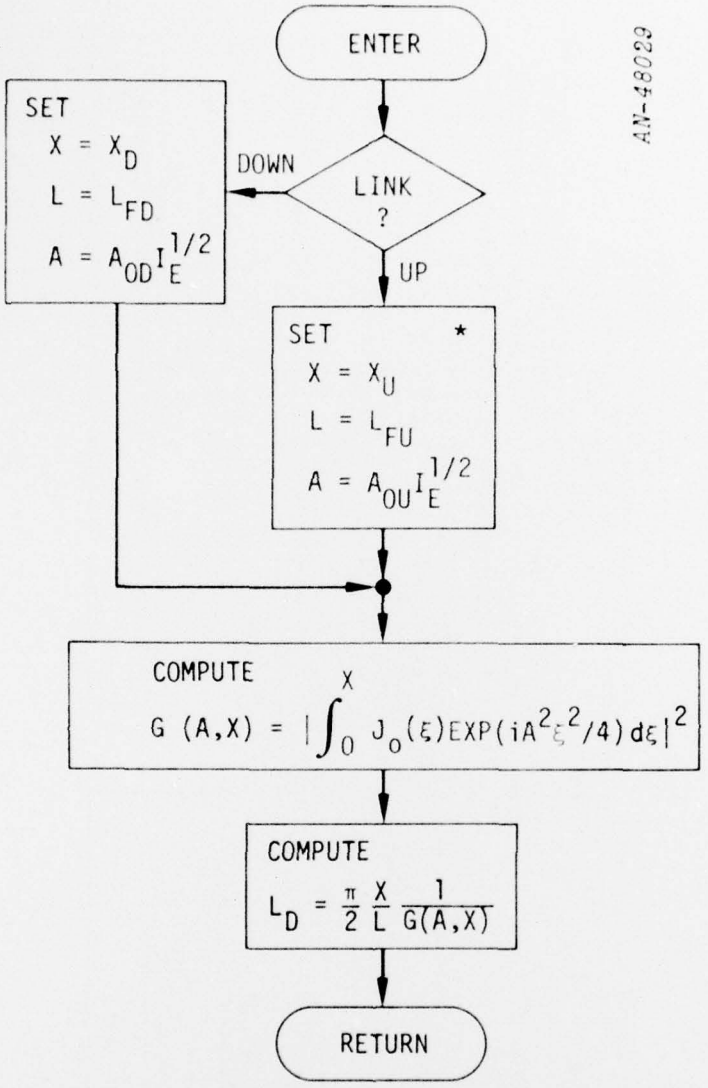

*X_U, X_D, L_{FU}, L_{FD} are real quantities which were computed in "INITIALIZATION".

$$A_{OU} = \frac{0.0585}{f_U^{3/2}\,\tau_U}\ ,\ A_{OD} = \frac{0.0585}{f_D^{3/2}\,\tau_D}$$

Figure B.11. Flow Diagram for Subroutine XLD--Computes Dispersive Loss

DISTRIBUTION LIST

DEPARTMENT OF DEFENSE

Director
Defense Advanced Rsch. Proj. Agency
ATTN: STO

Defense Communication Engineer Center
ATTN: Code R410, James W. McLean

Director
Defense Communications Agency
ATTN: Code 480

Defense Documentation Center
Cameron Station
12cy ATTN: TC

Director
Defense Nuclear Agency
ATTN: TISI, Archives
ATTN: DDST
ATTN: RAAE
3cy ATTN: TITL, Tech. Library

Dir. of Defense Rsch. & Engineering
ATTN: S&SS (OS)

Commander
Field Command
Defense Nuclear Agency
ATTN: FCPR

Director
Interservice Nuclear Weapons School
ATTN: Document Control

Director
Joint Strat. Tgt. Planning Staff, JCS
ATTN: JPST, Captain G. D. Goetz

Chief
Livermore Division Fld. Command, DNA
Lawrence Livermore Laboratory
ATTN: FCPRL

DEPARTMENT OF THE ARMY

Commander/Director
Atmospheric Sciences Laboratory
U.S. Army Electronics Command
ATTN: DRSEL-BL-SY-S, F. E. Niles

Director
BMD Advanced Tech. Ctr.
Huntsville Office
ATTN: ATC-T, Melvin T. Capps

Commander
Harry Diamond Laboratories
ATTN: DRXDO-NP, Francis N. Wimenitz
ATTN: DRXDO-TI
ATTN: DRXDO-NP

Director
TRASANA
ATTN: R. E. DeKinder, Jr.

DEPARTMENT OF THE ARMY (Continued)

Director
U.S. Army Ballistic Research Labs.
ATTN: Mark D. Kregel
ATTN: Lawrence J. Puckett

Commander
U.S. Army Foreign Science & Tech. Ctr.
ATTN: P. A. Crowley

Commander
U.S. Army Missile Command
ATTN: DRSMI-XS, Chief Scientist

Commander
U.S. Army Missile Intelligence Agency
ATTN: Jim Gamble

Commander
U.S. Army Nuclear Agency
ATTN: MONA-WE, J. Berberet

DEPARTMENT OF THE NAVY

Chief of Naval Operations
ATTN: Alexander Brandt

Commander
Naval Ocean Systems Center
3cy ATTN: Code 2200, Verne E. Hildebrand

Director
Naval Research Laboratory
ATTN: Code 7701, Jack D. Brown
ATTN: Code 7750, S. Ossakow

Officer-In-Charge
Naval Surface Weapons Center
ATTN: Code WX21, Tech. Lib.
ATTN: Code WA501, Navy Nuc. Prgms. Off.

Director
Strategic Systems Project Office
ATTN: NSSP-2722, Fred Wimberly
ATTN: NSP-2722, Marcus Meserole

DEPARTMENT OF THE AIR FORCE

AF Geophysics Laboratory, AFSC
ATTN: OPR, Harold Gardner
ATTN: OPR, James C. Ulwick
ATTN: OPR, Alva T. Stair

AF Weapons Laboratory, AFSC
ATTN: DYT, Capt L. Wittwer
ATTN: SUL
ATTN: NSS, John M. Kamm
ATTN: DYT, Capt Mark S. Fry

HQ USAF/RD
ATTN: RDQSM

Commander
Rome Air Development Center, AFSC
ATTN: EMTLD, Doc. Library

DEPARTMENT OF THE AIR FORCE (Continued)

SAMSO/SZ
ATTN: SZJ, Major Lawrence Doan

Commander In Chief
Strategic Air Command
ATTN: ADWATE, Capt Bruce Bauer
ATTN: XPFS, Maj Brian G. Stephan

Headquarters USAF/SA
ATTN: AFSA, Capt Henkle

ENERGY RESEARCH & DEVELOPMENT ADMINISTRATION

University of California
Lawrence Livermore Laboratory
ATTN: Ralph S. Hager, L-31
ATTN: Donald R. Dunn, L-156

Los Alamos Scientific Laboratory
ATTN: Doc. Con. for Eric Jones
ATTN: Doc. Con. for John Zinn

Sandia Laboratories
ATTN: Tech. Lib. Processes Station

OTHER GOVERNMENT AGENCY

Department of Commerce
Office of Telecommunications
Institute for Telecom. Science
ATTN: William F. Utlaut

DEPARTMENT OF DEFENSE CONTRACTORS

Aerospace Corporation
ATTN: Norman D. Stockwell
ATTN: Doug Rowcliffe

Brown Engineering Company, Inc.
Cummings Research Park
ATTN: Romeo A. Deliberis
ATTN: James E. Cato
ATTN: Joel D. Bigley

ESL, Inc.
ATTN: C. W. Prettie
ATTN: James Marshall

General Electric Company
Tempo-Center for Advanced Studies
ATTN: DASIAC
ATTN: Tim Stephens
ATTN: Warren S. Knapp

DEPARTMENT OF DEFENSE CONTRACTORS (Continued)

General Research Corporation
ATTN: John Ise, Jr.
ATTN: Joel Garbarino
ATTN: H. S. Ostrowsky
ATTN: J. J. Baltes

Jaycor
ATTN: S. R. Goldman

Johns Hopkins University
Applied Physics Laboratory
ATTN: Document Librarian

Lockheed Missiles & Space Co., Inc.
ATTN: D. R. Churchill

M.I.T. Lincoln Laboratory
ATTN: Lib. A-082 for David M. Towle

Martin Marietta Aerospace
Orlando Division
ATTN: Roy W. Heffner

Mission Research Corporation
ATTN: R. Hendrick
ATTN: R. Bogusch
ATTN: D. Sappenfield
ATTN: Russell Christian

Physical Dynamics, Inc.
ATTN: Joseph B. Workman

R & D Associates
ATTN: Bryan Gabbard
ATTN: Robert E. LeLevier

Science Applications, Inc.
ATTN: D. Sachs
ATTN: Curtis A. Smith
ATTN: Daniel A. Hamlin

Science Applications, Inc.
ATTN: Dale H. Divis
ATTN: Noel R. Byrn

Stanford Research Institute
ATTN: Walter G. Chesnut
ATTN: Ray L. Leadabrand

Visidyne, Inc.
ATTN: J. W. Carpenter
ATTN: Charles Humphrey